

Optimal Real-time Transmission Control for Spectrum Sharing between Cooperative Relay and Ad-hoc Networks

Yin Sun[†], Xiaofeng Zhong[†], Tsung-Hui Chang[‡], Shidong Zhou[†], Jing Wang[†], and Chong-Yung Chi[‡]

Abstract

Optimization based spectrum sharing strategies have been widely studied for various types of heterogeneous networks. However, the required computation and signaling process for implementing these optimal strategies usually result in significant control delay, making these strategies hardly be fulfilled in practical scenarios. This paper investigates optimal spectrum sharing strategies between a cooperative relay network (CRN) and a nearby ad-hoc network. Specifically, we optimize the spectrum access and resource allocation strategies of the CRN so that the average traffic collision time between the two networks can be minimized while maintaining a required throughput for the CRN. The development is first for a frame-level setting, and then is further extended to an ergodic setting. For the latter setting, we further propose an appealing real-time implementation method via Lagrangian dual optimization. The proposed method has quite small amount of real-time computation and negligible control delay, and thus is particularly suitable for practical implementations. Simulation results are presented to demonstrate the efficiency of the proposed strategies.

Index terms— Cognitive radio, relay network, ad-hoc network, resource allocation, spectrum access, spectrum sharing, collision prediction.

EDICS: WIN-CONT, WIN-RSMG, SPC-MULT, SPC-CRDS

The work of Yin Sun, Xiaofeng Zhong, Shidong Zhou, and Jing Wang was supported by National S&T Major Project (2010ZX03005-001-02), National Basic Research Program of China (2007CB310608), China's 863 Project (2009AA011501), National Natural Science Foundation of China (60832008) and Tsinghua Research Funding (2010THZ02-3). The work of Tsung-Hui Chang and Chong-Yung Chi is supported by National Science Council, Taiwan, under grant NSC-99-2221-E-007-052-MY3. This work was presented in part in IEEE ICC 2010 and IEEE ICC 2011.

[†]Yin Sun, Xiaofeng Zhong, Shidong Zhou, and Jing Wang are with the State Key Laboratory on Microwave and Digital Communications, Tsinghua National Laboratory for Information Science and Technology, and Department of Electronic Engineering, Tsinghua University, Beijing 100084, China. E-mail: sunyin02@gmail.com, {zhongxf,zhousd,wangj}@tsinghua.edu.cn.

[‡]Tsung-Hui Chang and Chong-Yung Chi are with Institute of Communications Engineering, and Department of Electrical Engineering, National Tsing Hua University, Hsinchu, Taiwan 30013. E-mail: tsunghui.chang@gmail.com, cychi@ee.nthu.edu.tw.

I. INTRODUCTION

In recent years, spectrum sharing between heterogeneous wireless networks has been recognized as a crucial technology for improving network spectrum efficiency [1], [2] and network capacity [3], [4]. There are two major models for spectrum sharing presently, namely, the *open sharing model* and the *hierarchical access model* [1], [2]. In the open sharing model, each of the coexisting networks has equal right to access the spectrum band, e.g., the unlicensed band, and there is no strict constraint on the interference level from one network to its neighbors. In the hierarchical access model which consists of a primary network and a secondary network, the secondary network, i.e., cognitive radio, dynamically accesses the spectrum provided that the primary users' transmission is almost not affected [1]. In either model, the imposed constraints on inter-network interference make spectrum sharing a challenging task [5], [6], especially when there is no explicit coordination between the coexisting networks.

To address this interference issue, cognitive spectrum access strategies have been proposed [7]–[14] for the hierarchical access model. While these works focus on MAC-layer spectrum access, there have been works focusing on physical-layer resource allocation of secondary networks, where strict constraints are imposed to limit the induced interference to the primary users; see [15]–[17] and also [18] for an overview. Joint optimization of the spectrum access and resource allocation has been proposed in [19] for an open sharing model that considers spectrum sharing between an uplink orthogonal frequency-division multiplexing (OFDM) system and an ad-hoc network.

However, some implementation issues were rarely considered in these optimization based spectrum sharing studies. First, real-time determination of the transmission parameters can be computationally quite demanding for realistic wireless communication systems [20]. Second, spectrum sensing and channel estimation are usually performed at spatially separate nodes, which requires information exchange between these nodes before solving the optimization problem. The resultant computation and signaling processes for deriving the optimal transmission solutions usually lead to significant control delay, making these strategies hardly be fulfilled in practical scenarios. Therefore, spectrum sharing strategies with little real-time calculation and small signaling delay are of great importance for practical applications.

In this paper, we study spectrum sharing between an uplink broadband cooperative relay network (CRN) and an ad-hoc network, as illustrated in Fig. 1. The CRN is composed of a source node (e.g., a mobile terminal), a relay, and a distant destination (e.g., a base station (BS)). The CRN adopts a two-phase transmission protocol for each transmission frame: in the first phase, the source broadcasts an information message to the relay and BS; in the second phase, the relay employs a broadband decode-and-forward

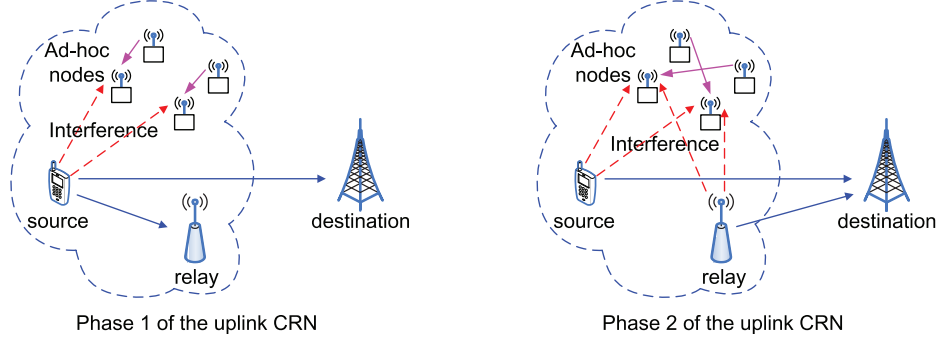


Fig. 1. System diagram of coexistence between a cooperative relay network (CRN) and an ad-hoc network. In Phase 1 (left plot), the source node broadcasts information to the relay and destination, and the transmitted signal interferes with the nearby ad-hoc links; in Phase 2 (right plot), the source and relay transmit signals to the destination simultaneously and both transmitted signals interfere with the ad-hoc links.

(DF) strategy [21]–[24] to forward the message. The source will transmit a new message to the BS in the second phase as well. In order to communicate with the distant BS, the source and relay transmit signals with peak powers, which, however, will induce strong interference to the nearby ad-hoc links operating over the same spectrum band. The ad-hoc transmitters, e.g., wireless sensor nodes, have relatively low transmission powers due to their short communication ranges, and thus their interference to the relay and destination can be treated as noise. Such an asymmetrical interference scenario is known as the “near-far effect” [3]. Our contributions in this paper are summarized as follows:

- 1) We first consider the case that the source and relay nodes perform spectrum sensing at the start of each frame. By modeling the ad-hoc traffic in each ad hoc band as independent binary continuous-time Markov chains (CTMC) [25], the average traffic collision time between the two networks can be obtained based on collision prediction. We formulate a frame-level transmission control problem that jointly optimizes physical-layer resource allocation and MAC-layer cognitive spectrum access of the CRN such that the average traffic collision time is minimized, subject to an uplink throughput requirement for the CRN.
- 2) The formulated design problem is a difficult nonconvex optimization problem with no closed-form expression for the objective function. We first derive the optimal spectrum access strategy, based on which, we show that the resource allocation problem can be reformulated as a convex optimization problem. To solve this problem in a low-complexity manner, we present a Lagrangian dual optimization method, which has a linear complexity with respect to the number of sub-channels.

- 3) As common issues of existing frame-level spectrum sharing strategies, the developed frame-level transmission control strategy requires excessive computation and signaling process, which may cause considerable control delay and is not suitable for real-time implementations. To overcome these issues, we further formulate an *ergodic* transmission control problem based on a long term average CRN achievable rate and a long term average traffic collision time. By exploiting the Lagrangian dual optimization solution, we develop a low-complexity, real-time implementation method for obtaining the optimal transmission control strategy. The proposed implementation method is appealing because most computation tasks are accomplished off-line, leaving only simple tasks for real-time computations. In addition, the signaling procedure and computation process are carefully designed to maximally reduce the transmission control delay. This method can accommodate an additional spectrum sensing in Phase 2 of each frame to further improve the performance of collision mitigation.

The transmission control proposed in this paper differs from that reported in [19] in three aspects: First, our interference metric and spectrum access strategy are more practical in the considered strong interference scenarios (to be presented in Remark 1 in Section III-A for more details). Second, the transmission control problem of our DF based CRN is more difficult compared to that of the one-hop uplink system considered in [19]. Finally, an optimal real-time implementation method is proposed for the ergodic transmission control strategy, which is never reported in the literature before.

The proposed designs may provide potential solutions for the coexistence problems of various heterogeneous wireless networks over open shared spectrum bands; e.g., the coexistence between unlicensed WiMAX (IEEE 802.16) and WiFi (IEEE 802.11) [26], the coexistence between a relay-assisted cellular network and ad-hoc networks including mobile ad-hoc networks [20] and peer-to-peer communication networks [27], and, in the domain of military communications, the coexistence between the broadband tactical backbone network and local sensor networks and tactical mobile ad-hoc networks [28].

For ease of later use, let us define the following notations: The probability of event A is denoted by $\Pr\{A\}$, and the probability of event A conditioned on event B is denoted by $\Pr\{A|B\}$. The indicator function of event A is given by $\mathbf{1}(A)$. $\mathbb{E}_\omega\{X\}$ represents expectation of X over random variable ω , and $\mathbb{E}\{X|Z = z\}$ is the conditional expectation of X given $Z = z$. We denote $\|\mathbf{x}\|_2$ as the Euclidean norm of vector \mathbf{x} , and denote $\pi(S)$ as the size (measure) of a set, e.g., $\pi([a, b]) = b - a$.

The remaining parts of this paper are organized as follows: In Section II, the system description and the formulation of frame-level transmission control problem are presented. Section III presents a Lagrangian optimization method to resolve the frame-level transmission control problem. The ergodic transmission

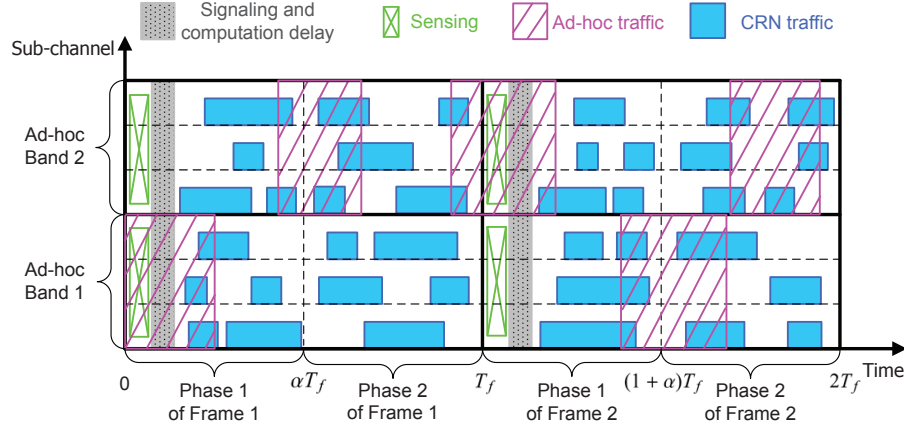


Fig. 2. Time-frequency transmission structure of the CRN and the ad-hoc network. In this figure, the number of CRN sub-channels is 6 ($N = 6$) and the number of ad-hoc bands is 2 ($M = 2$).

control problem and its real-time implementation method are presented in Section IV. Conclusions are drawn in Section V.

II. SYSTEM DESCRIPTION AND PROBLEM FORMULATION

A. Signal Model

We assume that the CRN employs a broadband multi-carrier air interface, where all nodes transmit and receive signals over N parallel sub-channels, denoted by $\mathcal{N} = \{1, 2, \dots, N\}$. The term “sub-channel” here represents either a frequency subband or a group of subcarriers in OFDM systems [1]. The ad-hoc links operate in M non-overlapped frequency bands, denoted by $\mathcal{M} = \{1, \dots, M\}$. Moreover, the m th ad-hoc band overlaps with the sub-channels of the CRN in the set $\mathcal{N}_m \subseteq \mathcal{N}$ for $m = 1, \dots, M$, where \mathcal{N}_m satisfies $\bigcup_{m=1}^M \mathcal{N}_m = \mathcal{N}$ and $\mathcal{N}_p \cap \mathcal{N}_q = \emptyset$ for $p \neq q$. An example with $M = 2$ and $N = 6$ is illustrated in Fig. 2.

In the temporal domain, all nodes in the CRN transmit and receive signals in a frame-by-frame manner, where each frame has a fixed duration T_f . The source node performs spectrum sensing at the start of each frame to detect the ACTIVE/IDLE state of each ad-hoc band. Perfect sensing and negligible sensing overhead is assumed in this paper, which is reasonable for moderate sensing signal-to-noise ratio (SNR) and common frame duration T_f ¹. Since the computation capability of the source node is quite limited, the

¹This assumption was confirmed in [10] for a WLAN energy detector. When the sensing SNR is 5 dB, a sensing duration of less than $5\mu\text{s}$ is sufficient to achieve a detection error probability of 10^{-5} . If we choose a frame duration from $500\mu\text{s}$ to 2ms , the sensing overhead is fairly small.

source node cannot determine the optimal transmission parameters. Therefore, it forwards the obtained sensing results to the destination. The destination node determines the optimal spectrum access and resource allocation strategies of the CRN, and feeds them back to the source and relay nodes. As one may have noticed, the solution computation and information signaling may cause non-negligible control delay between spectrum sensing and data transmission. In this work, we will explicitly take into account this control delay in the transmission control design. As illustrated in Fig. 2, we use δT_f to denote this control delay. In section IV, a real-time transmission control strategy with negligible δT_f will be presented.

In practice, the relay node operates in a half-duplex mode [21]. Therefore, each frame consists of 2 phases: In Phase 1, the source transmits signal to the relay and destination via a broadcast channel; in Phase 2, the source transmits a new information message, and, at the same time, the relay uses the DF relaying strategy to forward the information message received in Phase 1 to the destination, which forms a multiple-access channel. These scenarios are illustrated in Fig. 1. The time durations of Phase 1 and Phase 2 are set to αT_f and $(1 - \alpha)T_f$, respectively, where $\alpha \in (0, 1)$.

We assume that the source and relay nodes can switch on and off their transmissions *freely* over each sub-channel. Let $\mathbb{I}_n^{(1)} \subseteq [\delta T_f, \alpha T_f]$ denote the set of transmission time of the source over sub-channel n in Phase 1, and $\mathbb{I}_n^{(2)} \subseteq [\alpha T_f, T_f]$ denote that of the source and relay in Phase 2, for $n = 1, \dots, N$. Note that the source node cannot transmit during the time interval $[0, \delta T_f]$, owing to computation and signaling delay mentioned previously. As the example in Fig. 2 shows, $\mathbb{I}_n^{(1)}$ and $\mathbb{I}_n^{(2)}$ each may be a union of several disjoint transmission time intervals. Thus, the two sets $\mathbb{I}_n^{(1)}$ and $\mathbb{I}_n^{(2)}$ determine the spectrum access strategies of the CRN. For convenience, let us define

$$\theta_n^{(1)} = \frac{\pi(\mathbb{I}_n^{(1)})}{T_f}, \quad \theta_n^{(2)} = \frac{\pi(\mathbb{I}_n^{(2)})}{T_f}, \quad (1)$$

which represent the transmission time fractions of the CRN in Phase 1 and 2, respectively.

We assume that the wireless channels of source-relay, source-destination, and relay-destination links are block-fading [29], which means that the channel coefficients remain static within each frame, and can change from one frame to another. Let $h_n^{i,j}$ denote the frequency response of sub-channel n between transmitter i and receiver j , where $i \in \{s, r\}$ and $j \in \{r, d\}$ ($i \neq j$), in which s, r, d stand for the source, relay and destination, respectively. The interference plus noise at the relay and destination are modeled as independent, zero mean, circularly symmetric complex Gaussian random variables, with N_n^r and N_n^d denoting the respective peak power spectral densities (PSD) over sub-channel n (i.e., the weak interference from the ad-hoc network to the CRN is treated as noise). Hence, the quality of the wireless links can

be characterized by the normalized channel power gains $g_n^{s,r} \triangleq |h_n^{s,r}|^2/N_n^r W$, $g_n^{s,d} \triangleq |h_n^{s,d}|^2/N_n^d W$, and $g_n^{r,d} \triangleq |h_n^{r,d}|^2/N_n^d W$, where W is the bandwidth of each sub-channel. For the DF based CRN shown in Fig. 1 with N parallel sub-channels, it has been shown in [21, Eq. (45)] that the following rate is achievable

$$R_{CRN} = W \min \left\{ \sum_{n=1}^N \left[\theta_n^{(1)} \log_2 \left(1 + \frac{P_{s,n}^{(1)} \max\{g_n^{s,r}, g_n^{s,d}\}}{\theta_n^{(1)}} \right) + \theta_n^{(2)} \log_2 \left(1 + \frac{P_{s,n}^{(2)} g_n^{s,d}}{\theta_n^{(2)}} \right) \right], \right. \\ \left. \sum_{n=1}^N \left[\theta_n^{(1)} \log_2 \left(1 + \frac{P_{s,n}^{(1)} g_n^{s,d}}{\theta_n^{(1)}} \right) + \theta_n^{(2)} \log_2 \left(1 + \frac{P_{s,n}^{(2)} g_n^{s,d} + P_{r,n} g_n^{r,d}}{\theta_n^{(2)}} \right) \right] \right\}, \quad (2)$$

where $P_{s,n}^{(1)}$ and $P_{s,n}^{(2)}$ denote the total transmission powers of the source over sub-channel n in Phase 1 and Phase 2, respectively; and $P_{r,n}$ is the total transmission power of the relay over sub-channel n in Phase 2. The achievable rate R_{CRN} in (2) is a concave function of the transmission power and time variables $\{P_{s,n}^{(1)}, P_{s,n}^{(2)}, P_{r,n}, \theta_n^{(1)}, \theta_n^{(2)}, n \in \mathcal{N}\}$ according to [30, p. 89].

The ad-hoc traffic over the m th band is modeled as an independent, stationary binary CTMC $X_m(t)$, where $X_m(t) = 1$ ($X_m(t) = 0$) represents an ACTIVE (IDLE) state at time t . The holding periods of both ACTIVE and IDLE states are exponentially distributed with rate parameters λ_m and μ_m , respectively. The probability transition matrix of the CTMC model of band m is given by [25, p. 391]

$$P_m(t) = \frac{1}{\lambda_m + \mu_m} \begin{bmatrix} \mu_m + \lambda_m e^{-(\lambda_m + \mu_m)t} & \lambda_m - \lambda_m e^{-(\lambda_m + \mu_m)t} \\ \mu_m - \mu_m e^{-(\lambda_m + \mu_m)t} & \lambda_m + \mu_m e^{-(\lambda_m + \mu_m)t} \end{bmatrix}, \quad (3)$$

where the element in the i th row and j th column of $P_m(t)$ stands for the transition probability $\Pr\{X_m(t + \tau) = j - 1 | X_m(\tau) = i - 1\}$ for $i, j \in \{1, 2\}$. This CTMC model has been used and verified in many spectrum sharing studies including theoretical analysis and hardware tests; see [9]–[13], [19]. In practice, the parameters λ_m and μ_m can be estimated at the CRN nodes by monitoring the ad-hoc traffic in idle frames [9].

B. Traffic Collision Prediction and Interference Metric

Now let us derive the average traffic collision time between the CRN and the ad-hoc network. Since the ad-hoc nodes are in the vicinity of the source and relay nodes, the ad-hoc links would suffer from communication errors, whenever the CRN traffic happens to collide with the ad-hoc traffic ². Let $x_m \in$

²In general, the transmission error probability of one ad-hoc band is an increasing function of the average traffic collision time. In particular, if the ad-hoc transmission is uncoded in the physical layer or the duration of each ad-hoc code block is quite short, the ad-hoc transmission error probability is approximately proportional to the average traffic collision time [10]. Hence, the average traffic collision time can reflect the degrees that the ad-hoc traffic is disrupted.

$\{0, 1\}$ denote the sensing outcome for the m th ad-hoc band, i.e., $X_m(0) = x_m$. Given x_m , one can predict the average collision time based on the CTMC model in (3). Specifically, the average traffic collision time over the m th ad-hoc band is given by

$$\mathbb{E} \left\{ \int_{\bigcup_{n \in \mathcal{N}_m} \mathbb{I}_n^{(1)}} \mathbf{1}(X_m(t) = 1) dt + \int_{\bigcup_{n \in \mathcal{N}_m} \mathbb{I}_n^{(2)}} \mathbf{1}(X_m(t) = 1) dt \middle| X_m(0) = x_m \right\}. \quad (4)$$

It is worthwhile to note that the term $\bigcup_{n \in \mathcal{N}_m} \mathbb{I}_n^{(i)}$ in (4) is the union of all the CRN transmission time sets over the sub-channels \mathcal{N}_m . This term $\bigcup_{n \in \mathcal{N}_m} \mathbb{I}_n^{(i)}$ reflects the fact that, in the considered strong interference scenario, the ad-hoc transmission in the m th band is disrupted even if the CRN only transmits in one sub-channel $n \in \mathcal{N}_m$.

Each of the expectation terms in (4) can be calculated as follows

$$\begin{aligned} \mathbb{E} \left\{ \int_{\bigcup_{n \in \mathcal{N}_m} \mathbb{I}_n^{(i)}} \mathbf{1}(X_m(t) = 1) dt \middle| X_m(0) = x_m \right\} &= \int_{\bigcup_{n \in \mathcal{N}_m} \mathbb{I}_n^{(i)}} \mathbb{E} \{X_m(t) = 1 | X_m(0) = x_m\} dt \\ &= \int_{\bigcup_{n \in \mathcal{N}_m} \mathbb{I}_n^{(i)}} \Pr \{X_m(t) = 1 | X_m(0) = x_m\} dt. \end{aligned} \quad (5)$$

By (5), the total traffic collision time summed over all the ad-hoc bands is given by

$$I = \sum_{m=1}^M \left[\int_{\bigcup_{n \in \mathcal{N}_m} \mathbb{I}_n^{(1)}} \Pr \{X_m(t) = 1 | X_m(0) = x_m\} dt + \int_{\bigcup_{n \in \mathcal{N}_m} \mathbb{I}_n^{(2)}} \Pr \{X_m(t) = 1 | X_m(0) = x_m\} dt \right]. \quad (6)$$

C. Problem Formulation of Transmission Control

The goal of the CRN is to control the source and relay's transmission powers $P_{s,n}^{(1)}, P_{s,n}^{(2)}$ and $P_{r,n}$, and their spectrum access strategies $\mathbb{I}_n^{(1)}$ and $\mathbb{I}_n^{(2)}$, such that the total traffic collision time in (6) is minimized, while a minimum uplink throughput R_{\min} can be maintained. The considered joint spectrum access and resource allocation problem can be formulated as the following optimization problem:

$$(P) \quad \min_{P_{s,n}^{(1)}, P_{s,n}^{(2)}, P_{r,n}, \mathbb{I}_n^{(1)}, \mathbb{I}_n^{(2)}, n=1, \dots, N} \frac{I}{T_f} \quad (7a)$$

$$\text{s.t.} \quad R_{CRN} \geq R_{\min}, \quad (7b)$$

$$\sum_{n=1}^N [P_{s,n}^{(1)} + P_{s,n}^{(2)}] \leq P_{\max}^s, \quad \sum_{n=1}^N P_{r,n} \leq P_{\max}^r, \quad (7c)$$

$$P_{s,n}^{(1)}, P_{s,n}^{(2)}, P_{r,n} \geq 0, \quad n = 1, \dots, N, \quad (7d)$$

$$\mathbb{I}_n^{(1)} \subseteq [\delta T_f, \alpha T_f], \quad \mathbb{I}_n^{(2)} \subseteq [\alpha T_f, T_f], \quad n = 1, \dots, N, \quad (7e)$$

$$\pi(\mathbb{I}_n^{(1)}) = \theta_n^{(1)} T_f, \quad \pi(\mathbb{I}_n^{(2)}) = \theta_n^{(2)} T_f, \quad n = 1, \dots, N, \quad (7f)$$

where R_{CRN} and I are given by (2) and (6), respectively, (7f) follows from (1), and P_{\max}^s and P_{\max}^r in (7c) denote the power constraints on the source and relay nodes, respectively.

III. OPTIMAL TRANSMISSION CONTROL SOLUTION

Problem (P) is difficult to solve mainly because the objective function I has no closed-form expression in general. Fortunately, this issue can be resolved by analyzing the optimal sets $\mathbb{I}_n^{(1)}$ and $\mathbb{I}_n^{(2)}$, and Problem (P) can be reformulated as a convex optimization problem, as we will present in this section. A subgradient based Lagrangian optimization method is also proposed to efficiently obtain an optimal solution of (P).

A. Reformulation of Problem (P)

The key idea that makes this convex reformulation possible is to examine the optimal spectrum access $\mathbb{I}_n^{(1)}$ and $\mathbb{I}_n^{(2)}$ for Problem (P). In particular, it can be shown (in Lemma 1 below) that the optimal spectrum access must satisfy the following two principles:

- 1) In both Phase 1 and Phase 2, the source and relay nodes should transmit as soon (late) as possible if the sensing outcome is IDLE (ACTIVE);
- 2) The CRN should have identical spectrum access strategy for the sub-channels that overlap with a common ad-hoc band; that is, $\mathbb{I}_p^{(i)} = \mathbb{I}_q^{(i)}$ for all $p, q \in \mathcal{N}_m$, where $m \in \mathcal{M}$ and $i \in \{1, 2\}$.

Principle 2) is in the flavor of the interference alignment technique in [31] since both of them align the transmissions in order to reduce the interference to the ad-hoc links. Let us define

$$\hat{\theta}_m^{(i)} \triangleq \max \left\{ \theta_n^{(i)}, n \in \mathcal{N}_m \right\} \quad (8)$$

as the largest transmission time fractions over the sub-channels \mathcal{N}_m in phase i . The optimal spectrum access strategy is given by following lemma, which is proved in Appendix A.

Lemma 1 For any given transmission time fractions $\{\hat{\theta}_m^{(1)} \in [0, \alpha - \delta], \hat{\theta}_m^{(2)} \in [0, 1 - \alpha]\}_{m=1}^M$ and transmission power $\{P_{s,n}^{(1)}, P_{s,n}^{(2)}, P_{r,n}\}_{n=1}^N$ in Problem (P), we have that:

- 1) The optimal spectrum access strategy in Phase 1 is given by $\mathbb{I}_n^{(1)} = [\delta T_f, (\delta + \hat{\theta}_m^{(1)})T_f]$ for all $n \in \mathcal{N}_m$ if the sensing outcome is $x_m = 0$, and is given by $\mathbb{I}_n^{(1)} = [(\alpha - \hat{\theta}_m^{(1)})T_f, \alpha T_f]$ for all $n \in \mathcal{N}_m$ if the sensing outcome is $x_m = 1$;
- 2) The optimal spectrum access strategy in Phase 2 is given by $\mathbb{I}_n^{(2)} = [\alpha T_f, (\alpha + \hat{\theta}_m^{(2)})T_f]$ for all $n \in \mathcal{N}_m$ if the sensing outcome is $x_m = 0$, and is given by $\mathbb{I}_n^{(2)} = [(1 - \hat{\theta}_m^{(2)})T_f, T_f]$ for all $n \in \mathcal{N}_m$ if the sensing outcome is $x_m = 1$.

An example that illustrates the spectrum access strategy of Lemma 1 is shown in Fig. 3.

Remark 1: A similar result of Lemma 1 was reported in [19] for a different interference metric, which cumulates the traffic collisions for all the sub-channels within one ad-hoc band. For example, $\sum_{n \in \mathcal{N}_m} \mathbb{E} \left\{ \int_{\mathbb{I}_n^{(i)}} X_m(t) dt \middle| X_m(0) = x_m \right\}$ is defined as the average traffic collision time over the m th ad-hoc band in [19] instead of the one given in (5). Our interference metric is more practical than that reported in [19], because, in strong interference scenario, the ad-hoc transmission in the m th band is interrupted even if the CRN only transmits in one sub-channel $n \in \mathcal{N}_m$. In Appendix A, we show that the sub-channels in \mathcal{N}_m should align their transmissions to reduce the interference to the ad-hoc links, which was not considered in [19]. Such a difference can be observed by comparing Fig. 3 with [19, Fig. 1].

According to Lemma 1, the integration region in each term of (6) can be simply expressed as a time interval. In order to simplify (6), we define for $\theta \in [0, \alpha - \delta]$,

$$\begin{aligned} \phi_{(1)}(\theta; x_m = 0) &= \int_{[\delta T_f, (\delta + \theta)T_f]} \Pr(X_m(t) = 1 | X_m(0) = 0) dt \\ &= \frac{\lambda_m}{\lambda_m + \mu_m} \left\{ \theta + \frac{1}{(\lambda_m + \mu_m)T_f} e^{-(\lambda_m + \mu_m)\delta T_f} \left[e^{-(\lambda_m + \mu_m)\theta T_f} - 1 \right] \right\} T_f, \end{aligned} \quad (9)$$

$$\begin{aligned} \phi_{(1)}(\theta; x_m = 1) &= \int_{[(\alpha - \theta)T_f, \alpha T_f]} \Pr(X_m(t) = 1 | X_m(0) = 1) dt \\ &= \frac{\lambda_m}{\lambda_m + \mu_m} \left\{ \theta + \frac{\mu_m}{\lambda_m} \frac{1}{(\lambda_m + \mu_m)T_f} e^{-(\lambda_m + \mu_m)\alpha T_f} \left[e^{(\lambda_m + \mu_m)\theta T_f} - 1 \right] \right\} T_f, \end{aligned} \quad (10)$$

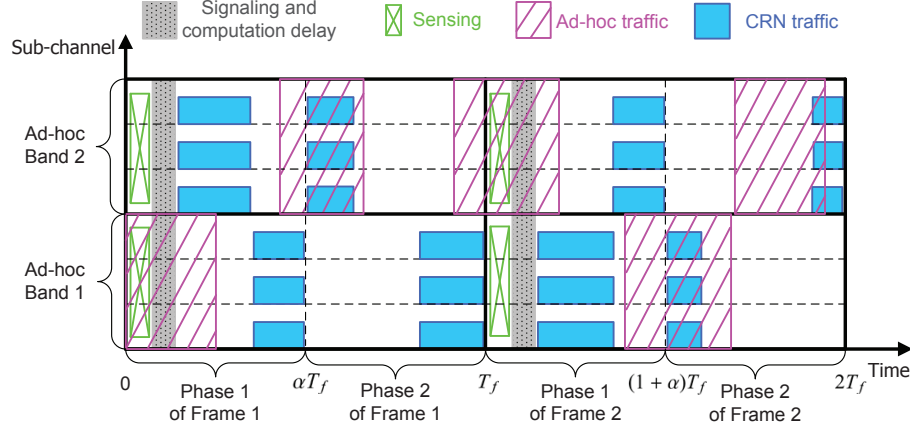


Fig. 3. An example illustrating the spectrum access strategy of Lemma 1. The sensing outcomes of frame 1 are $x_1 = 1$ and $x_2 = 0$, and the sensing outcomes of frame 2 are $x_1 = 0$ and $x_2 = 1$.

and define for $\theta \in [0, 1 - \alpha]$,

$$\begin{aligned} \phi_{(2)}(\theta; x_m = 0) &= \int_{[\alpha T_f, (\theta + \alpha)T_f]} \Pr(X_m(t) = 1 | X_m(0) = 0) dt \\ &= \frac{\lambda_m}{\lambda_m + \mu_m} \left\{ \theta + \frac{1}{(\lambda_m + \mu_m)T_f} e^{-(\lambda_m + \mu_m)\alpha T_f} \left[e^{-(\lambda_m + \mu_m)\theta T_f} - 1 \right] \right\} T_f, \end{aligned} \quad (11)$$

$$\begin{aligned} \phi_{(2)}(\theta; x_m = 1) &= \int_{[T_f - \theta T_f, T_f]} \Pr(X_m(t) = 1 | X_m(0) = 1) dt \\ &= \frac{\lambda_m}{\lambda_m + \mu_m} \left\{ \theta + \frac{\mu_m}{\lambda_m} \frac{1}{(\lambda_m + \mu_m)T_f} e^{-(\lambda_m + \mu_m)T_f} \left[e^{(\lambda_m + \mu_m)\theta T_f} - 1 \right] \right\} T_f. \end{aligned} \quad (12)$$

The computation and signaling delay δT_f compromise the performance of spectrum access strategy in Lemma 1, as $\phi_{(1)}(\theta; 0)$ is strictly increasing in δ . Then, the interference metric in (6) can be simplified as

$$I = \sum_{m=1}^M \left[\phi_{(1)}(\hat{\theta}_m^{(1)}; x_m) + \phi_{(2)}(\hat{\theta}_m^{(2)}; x_m) \right]. \quad (13)$$

It is easy to verify that the functions $\phi_{(1)}(\theta; x)$ and $\phi_{(2)}(\theta; x)$ in (9)-(12) are strictly increasing and strictly convex functions of θ . Thus I in (13) is a convex function of $\hat{\theta}_m^{(1)}$ and $\hat{\theta}_m^{(2)}$.

On the other hand, it follows from (2), (8) and Lemma 1 that the constraint (7b) of (P) can be equivalently expressed as

$$R_1 \geq R_{\min}, \quad R_2 \geq R_{\min}, \quad (14)$$

where

$$R_1 = W \sum_{m \in \mathcal{M}} \sum_{n \in \mathcal{N}_m} \left[\hat{\theta}_m^{(1)} \log_2 \left(1 + \frac{P_{s,n}^{(1)} \max\{g_n^{s,r}, g_n^{s,d}\}}{\hat{\theta}_m^{(1)}} \right) + \hat{\theta}_m^{(2)} \log_2 \left(1 + \frac{P_{s,n}^{(2)} g_n^{s,d}}{\hat{\theta}_m^{(2)}} \right) \right], \quad (15)$$

$$R_2 = W \sum_{m \in \mathcal{M}} \sum_{n \in \mathcal{N}_m} \left[\hat{\theta}_m^{(1)} \log_2 \left(1 + \frac{P_{s,n}^{(1)} g_n^{s,d}}{\hat{\theta}_m^{(1)}} \right) + \hat{\theta}_m^{(2)} \log_2 \left(1 + \frac{P_{s,n}^{(2)} g_n^{s,d} + P_{r,n} g_n^{r,d}}{\hat{\theta}_m^{(2)}} \right) \right]. \quad (16)$$

By (13) and (14), Problem (P) is equivalent with the following problem:

$$\min_{\substack{P_{s,n}^{(1)}, P_{s,n}^{(2)}, P_{r,n}, \hat{\theta}_m^{(1)}, \hat{\theta}_m^{(2)}, \\ n=1, \dots, N, m=1, \dots, M}} \frac{1}{T_f} \sum_{m=1}^M \left[\phi_{(1)} \left(\hat{\theta}_m^{(1)}; x_m \right) + \phi_{(2)} \left(\hat{\theta}_m^{(2)}; x_m \right) \right] \quad (17a)$$

$$\text{s.t.} \quad R_1 \geq R_{\min} \quad (17b)$$

$$R_2 \geq R_{\min} \quad (17c)$$

$$\sum_{n=1}^N \left[P_{s,n}^{(1)} + P_{s,n}^{(2)} \right] \leq P_{\max}^s \quad (17d)$$

$$\sum_{n=1}^N P_{r,n} \leq P_{\max}^r \quad (17e)$$

$$P_{s,n}^{(1)}, P_{s,n}^{(2)}, P_{r,n} \geq 0, \quad n = 1, \dots, N \quad (17f)$$

$$0 \leq \hat{\theta}_m^{(1)} \leq \alpha - \delta, \quad 0 \leq \hat{\theta}_m^{(2)} \leq 1 - \alpha, \quad m = 1, \dots, M, \quad (17g)$$

which is a convex optimization problem. While problem (17) can be solved by interior-point methods, we present in the next subsection a low-complexity Lagrangian optimization method.

B. Lagrangian Optimization Method for Problem (17)

Suppose that problem (17) is strictly feasible. Then, according to the Slater's condition [30], the strong duality holds for (17). Hence we can alternatively consider the following dual optimization problem

$$\max_{\zeta, \sigma, \varepsilon, \eta \geq 0} \left\{ \min_{(P_{s,n}^{(1)}, P_{s,n}^{(2)}, P_{r,n}, \hat{\theta}_m^{(1)}, \hat{\theta}_m^{(2)}) \in \mathcal{V}} L \right\}, \quad (18)$$

where $\mathcal{V} \triangleq \left\{ (P_{s,n}^{(1)}, P_{s,n}^{(2)}, P_{r,n}, \hat{\theta}_m^{(1)}, \hat{\theta}_m^{(2)}) \mid 0 \leq \hat{\theta}_m^{(1)} \leq \alpha - \delta, 0 \leq \hat{\theta}_m^{(2)} \leq 1 - \alpha, P_{s,n}^{(1)}, P_{s,n}^{(2)}, P_{r,n} \geq 0, n \in \mathcal{N}, m \in \mathcal{M} \right\}$,

$$\begin{aligned} L = & \frac{1}{T_f} \sum_{m=1}^M \left[\phi_{(1)} \left(\hat{\theta}_m^{(1)}; x_m \right) + \phi_{(2)} \left(\hat{\theta}_m^{(2)}; x_m \right) \right] + \frac{\zeta}{W} (R_{\min} - R_1) + \frac{\sigma}{W} (R_{\min} - R_2) \\ & + \varepsilon \left[\sum_{n=1}^N (P_{s,n}^{(1)} + P_{s,n}^{(2)}) - P_{\max}^s \right] + \eta \left[\sum_{n=1}^N P_{r,n} - P_{\max}^r \right], \end{aligned} \quad (19)$$

is the partial Lagrangian [32] of (17), $\zeta \geq 0$, $\sigma \geq 0$, $\varepsilon \geq 0$, and $\eta \geq 0$ are the dual variables associated with the constraints (17b), (17c), (17d), and (17e), respectively. As will be shown, the inner minimization problem of (18) has closed-form solutions for $P_{s,n}^{(1)}$, $P_{s,n}^{(2)}$ and $P_{r,n}$ for $n = 1, \dots, N$, and $\hat{\theta}_m^{(1)}$ and $\hat{\theta}_m^{(2)}$ for $m = 1, \dots, M$. Hence, the computational complexity for solving the inner problem is only linear with respect to N and M . Moreover, the outer maximization problem of (18) only involves four optimization variables $(\zeta, \sigma, \varepsilon, \eta)$, which is much smaller than the number of variables of the primal problem (17).

Suppose that a dual variable $\nu \triangleq (\zeta, \sigma, \varepsilon, \eta)^T$ is given. Let us present the closed-form solutions of the inner minimization problem of (18). Because the inner problem is convex, the optimal $(P_{s,n}^{(1)}, P_{s,n}^{(2)}, P_{r,n}, \hat{\theta}_m^{(1)}, \hat{\theta}_m^{(2)})$ for fixed dual variable ν must satisfy the Karush-Kuhn-Tucker (KKT) conditions [30] of the inner problem, which can be expressed as:

$$\frac{\partial L}{\partial P_{s,n}^{(1)}} = -\frac{\zeta \max\{g_n^{s,r}, g_n^{s,d}\}}{\left(1 + \max\{g_n^{s,r}, g_n^{s,d}\} \frac{P_{s,n}^{(1)}}{\hat{\theta}_m^{(1)}}\right) \ln 2} - \frac{\sigma g_n^{s,d}}{\left(1 + g_n^{s,d} \frac{P_{s,n}^{(1)}}{\hat{\theta}_m^{(1)}}\right) \ln 2} + \varepsilon \begin{cases} = 0 & \text{if } P_{s,n}^{(1)} > 0 \\ \geq 0 & \text{if } P_{s,n}^{(1)} = 0 \end{cases} \quad (20)$$

$$\frac{\partial L}{\partial P_{s,n}^{(2)}} = -\frac{\zeta g_n^{s,d}}{\left(1 + g_n^{s,d} \frac{P_{s,n}^{(2)}}{\hat{\theta}_m^{(2)}}\right) \ln 2} - \frac{\sigma g_n^{s,d}}{\left(1 + g_n^{s,d} \frac{P_{s,n}^{(2)}}{\hat{\theta}_m^{(2)}} + g_n^{r,d} \frac{P_{r,n}}{\hat{\theta}_m^{(2)}}\right) \ln 2} + \varepsilon \begin{cases} = 0 & \text{if } P_{s,n}^{(2)} > 0 \\ \geq 0 & \text{if } P_{s,n}^{(2)} = 0 \end{cases} \quad (21)$$

$$\frac{\partial L}{\partial P_{r,n}} = -\frac{\sigma g_n^{r,d}}{\left(1 + g_n^{s,d} \frac{P_{s,n}^{(2)}}{\hat{\theta}_m^{(2)}} + g_n^{r,d} \frac{P_{r,n}}{\hat{\theta}_m^{(2)}}\right) \ln 2} + \eta \begin{cases} = 0 & \text{if } P_{r,n} > 0 \\ \geq 0 & \text{if } P_{r,n} = 0 \end{cases} \quad (22)$$

$$\frac{\partial L}{\partial \hat{\theta}_m^{(1)}} = -\zeta \sum_{n \in \mathcal{N}_m} f\left(\max\{g_n^{s,r}, g_n^{s,d}\} \frac{P_{s,n}^{(1)}}{\hat{\theta}_m^{(1)}}\right) - \sigma \sum_{n \in \mathcal{N}_m} f\left(g_n^{s,d} \frac{P_{s,n}^{(1)}}{\hat{\theta}_m^{(1)}}\right) + \frac{\partial \phi_{(1)}(\hat{\theta}_m^{(1)}; x_m)}{\partial \hat{\theta}_m^{(1)}} \begin{cases} \leq 0 & \text{if } \hat{\theta}_m^{(1)} = \alpha - \delta \\ = 0 & \text{if } \hat{\theta}_m^{(1)} \in (0, \alpha - \delta) \\ \geq 0 & \text{if } \hat{\theta}_m^{(1)} = 0 \end{cases} \quad (23)$$

$$\frac{\partial L}{\partial \hat{\theta}_m^{(2)}} = -\zeta \sum_{n \in \mathcal{N}_m} f\left(g_n^{s,d} \frac{P_{s,n}^{(2)}}{\hat{\theta}_m^{(2)}}\right) - \sigma \sum_{n \in \mathcal{N}_m} f\left(g_n^{s,d} \frac{P_{s,n}^{(2)}}{\hat{\theta}_m^{(2)}} + g_n^{r,d} \frac{P_{r,n}}{\hat{\theta}_m^{(2)}}\right) + \frac{\partial \phi_{(2)}(\hat{\theta}_m^{(2)}; x_m)}{\partial \hat{\theta}_m^{(2)}} \begin{cases} \leq 0 & \text{if } \hat{\theta}_m^{(2)} = 1 - \alpha \\ = 0 & \text{if } \hat{\theta}_m^{(2)} \in (0, 1 - \alpha) \\ \geq 0 & \text{if } \hat{\theta}_m^{(2)} = 0 \end{cases} \quad (24)$$

where $f(x) \triangleq \log_2(1+x) - \frac{x}{(1+x)\ln 2}$ in (23) and (24).

We first solve (20) to obtain the optimal ratio $\frac{P_{s,n}^{(1)}}{\hat{\theta}_m^{(1)}}$. Specifically, if $P_{s,n}^{(1)} > 0$, then equality in (20) holds, and an optimal $\frac{P_{s,n}^{(1)}}{\hat{\theta}_m^{(1)}}$ is equal to the positive root x of the following quadratic equation

$$\frac{\zeta \max\{g_n^{s,r}, g_n^{s,d}\}}{1 + \max\{g_n^{s,r}, g_n^{s,d}\}x} + \frac{\sigma g_n^{s,d}}{1 + g_n^{s,d}x} = \varepsilon \ln 2. \quad (25)$$

If (20) has no positive root, then $\frac{P_{s,n}^{(1)}}{\hat{\theta}_m^{(1)}} = 0$. Next, let us find the optimal $\frac{P_{s,n}^{(2)}}{\hat{\theta}_m^{(2)}}$ and $\frac{P_{r,n}}{\hat{\theta}_m^{(2)}}$ by solving (21) and (22). If $P_{r,n} > 0$, the equality in (22) holds, and the optimal $\frac{P_{s,n}^{(2)}}{\hat{\theta}_m^{(2)}}$ and $\frac{P_{r,n}}{\hat{\theta}_m^{(2)}}$ can be obtained from

(21) and (22) as

$$\frac{P_{s,n}^{(2)}}{\hat{\theta}_m^{(2)}} = \left[\frac{\zeta}{(\varepsilon - \eta g_n^{s,d}/g_n^{r,d}) \ln 2} - \frac{1}{g_n^{s,d}} \right]^+, \quad (26)$$

$$\frac{P_{r,n}}{\hat{\theta}_m^{(2)}} = \frac{\sigma}{\eta \ln 2} - \frac{1}{g_n^{r,d}} - \frac{g_n^{s,d}}{g_n^{r,d}} \frac{P_{s,n}^{(2)}}{\hat{\theta}_m^{(2)}}, \quad (27)$$

where $[x]^+ = \max\{x, 0\}$. Instead, if $P_{r,n} = 0$, we obtain from (21) and (22) that

$$\frac{P_{s,n}^{(2)}}{\hat{\theta}_m^{(2)}} = \left[\frac{\zeta + \sigma}{\varepsilon \ln 2} - \frac{1}{g_n^{s,d}} \right]^+, \quad (28)$$

$$\frac{P_{r,n}}{\hat{\theta}_m^{(2)}} = 0, \quad (29)$$

where (28) is actually the water-filling solution when the source directly communicates with the destination without the use of relay.

The optimal $\hat{\theta}_m^{(1)}$ and $\hat{\theta}_m^{(2)}$ can be obtained by solving (23) and (24), respectively, provided that the optimal $\frac{P_{s,n}^{(1)}}{\hat{\theta}_m^{(1)}}$, $\frac{P_{s,n}^{(2)}}{\hat{\theta}_m^{(2)}}$ and $\frac{P_{r,n}}{\hat{\theta}_m^{(2)}}$ have been obtained from (25)-(29). By substituting $\frac{P_{s,n}^{(1)}}{\hat{\theta}_m^{(1)}}$, $\frac{P_{s,n}^{(2)}}{\hat{\theta}_m^{(2)}}$ and $\frac{P_{r,n}}{\hat{\theta}_m^{(2)}}$ into (23)-(24), and by the definitions of $\phi_{(1)}(\theta; x)$ and $\phi_{(2)}(\theta; x)$ in (9)-(12), we can obtain the optimal values of $\hat{\theta}_m^{(1)}$ and $\hat{\theta}_m^{(2)}$ as follows: For $x_m = 0$, we have ¹

$$\hat{\theta}_m^{(1)} = \min \left\{ \left[-\frac{1}{(\lambda_m + \mu_m)T_f} \ln \left\{ 1 - \frac{\lambda_m + \mu_m}{\lambda_m} \sum_{n \in \mathcal{N}_m} \left[\sigma f \left(g_n^{s,d} \frac{P_{s,n}^{(1)}}{\hat{\theta}_m^{(1)}} \right) + \zeta f \left(\max\{g_n^{s,r}, g_n^{s,d}\} \frac{P_{s,n}^{(1)}}{\hat{\theta}_m^{(1)}} \right) \right] \right\} - \delta \right]^+, \alpha - \delta \right\}, \quad (30)$$

$$\hat{\theta}_m^{(2)} = \min \left\{ \left[-\frac{1}{(\lambda_m + \mu_m)T_f} \ln \left\{ 1 - \frac{\lambda_m + \mu_m}{\lambda_m} \sum_{n \in \mathcal{N}_m} \left[\zeta f \left(g_n^{s,d} \frac{P_{s,n}^{(2)}}{\hat{\theta}_m^{(2)}} \right) + \sigma f \left(g_n^{s,d} \frac{P_{s,n}^{(2)}}{\hat{\theta}_m^{(2)}} + g_n^{r,d} \frac{P_{r,n}}{\hat{\theta}_m^{(2)}} \right) \right] \right\} - \alpha \right]^+, 1 - \alpha \right\}, \quad (31)$$

and for $x_m = 1$, we have

$$\hat{\theta}_m^{(1)} = \min \left\{ \left[\alpha + \frac{1}{(\lambda_m + \mu_m)T_f} \ln \left\{ \frac{\lambda_m + \mu_m}{\mu_m} \sum_{n \in \mathcal{N}_m} \left[\sigma f \left(g_n^{s,d} \frac{P_{s,n}^{(1)}}{\hat{\theta}_m^{(1)}} \right) + \zeta f \left(\max\{g_n^{s,r}, g_n^{s,d}\} \frac{P_{s,n}^{(1)}}{\hat{\theta}_m^{(1)}} \right) \right] - \frac{\lambda_m}{\mu_m} \right\} \right]^+, \alpha - \delta \right\}, \quad (32)$$

¹For the notational simplicity in (30)-(33), we have extended the definition of the natural logarithm $\ln(x)$ to that with $\ln(x) = -\infty$ for $x \in (-\infty, 0]$.

$$\hat{\theta}_m^{(2)} = \min \left\{ \left[1 + \frac{1}{(\lambda_m + \mu_m)T_f} \ln \left\{ \frac{\lambda_m + \mu_m}{\mu_m} \sum_{n \in \mathcal{N}_m} \left[\zeta f \left(g_n^{s,d} \frac{P_{s,n}^{(2)}}{\hat{\theta}_m^{(2)}} \right) + \sigma f \left(g_n^{s,d} \frac{P_{s,n}^{(2)}}{\hat{\theta}_m^{(2)}} + g_n^{r,d} \frac{P_{r,n}}{\hat{\theta}_m^{(2)}} \right) - \frac{\lambda_m}{\mu_m} \right] \right\}^+ , 1 - \alpha \right\}. \quad (33)$$

By substituting (30)-(33) into (25)-(29), the optimal $P_{s,n}^{(1)}, P_{s,n}^{(2)}, P_{r,n}$ can then be obtained.

Algorithm 1 The proposed Lagrangian optimization algorithm for solving (P)

- 1: **Input** the system parameters $(N, M, \alpha, P_{\max}^s, P_{\max}^r, T_f, R_{\min})$, the ad-hoc traffic parameters $\{\lambda_m, \mu_m\}_{m=1}^M$, the channel quality $\{g_n^{s,r}, g_n^{s,d}, g_n^{r,d}\}_{n=1}^N$, the sensing outcome $\{x_m\}_{m=1}^M$, the computation and signaling delay parameter δ , and a solution accuracy ϵ .
 - 2: Set the iteration number $k = 1$; initialize the dual variable $\boldsymbol{\nu}_1$.
 - 3: Compute the optimal $\{P_{s,n}^{(1)}, P_{s,n}^{(2)}, P_{r,n}\}_{n=1}^N$ and $\{\hat{\theta}_m^{(1)}, \hat{\theta}_m^{(2)}\}_{m=1}^M$ according to (25)-(33).
 - 4: Update the dual variable $\boldsymbol{\nu}_{k+1}$ according to (34) and (35).
 - 5: If $\|\boldsymbol{\nu}_{k+1} - \boldsymbol{\nu}_k\|_2 \leq \epsilon$, go to Step 6; otherwise, set $k = k + 1$ and return to Step 3.
 - 6: **Output** the optimal primal solution $\{P_{s,n}^{(1)}, P_{s,n}^{(2)}, P_{r,n}\}_{n=1}^N$ and $\{\hat{\theta}_m^{(1)}, \hat{\theta}_m^{(2)}\}_{m=1}^M$. The optimal spectrum access strategy $\{\mathbb{I}_n^{(1)}, \mathbb{I}_n^{(2)}\}_{n=1}^N$ can be obtained by Lemma 1.
-

What remains for solving (18) is to optimize the dual variable $\boldsymbol{\nu} = (\zeta, \sigma, \varepsilon, \eta)^T$ for the outer maximization problem. In view of that the dual function of (17) (the optimal value of the inner problem of (18)) may not be differentiable [33], we consider to update $\boldsymbol{\nu}$ using the subgradient method [34]. Specifically, at the k th iteration, the subgradient method updates $\boldsymbol{\nu}$ by [34]

$$\boldsymbol{\nu}_{k+1} = [\boldsymbol{\nu}_k + s_k \mathbf{h}(\boldsymbol{\nu}_k)]^+, \quad (34)$$

where the subscript k denotes the iteration number, s_k is the step size of the k th iteration, and $\mathbf{h}(\boldsymbol{\nu}_k)$ is the subgradient of the dual function, which is given by [33]

$$\mathbf{h}(\boldsymbol{\nu}_k) = \begin{bmatrix} (R_{\min} - R_1^*)/W \\ (R_{\min} - R_2^*)/W \\ \sum_{n=1}^N (P_{s,n}^{(1)*} + P_{s,n}^{(2)*}) - P_{\max}^s \\ \sum_{n=1}^N P_{r,n}^* - P_{\max}^r \end{bmatrix}, \quad (35)$$

where $P_{s,n}^{(1)*}, P_{s,n}^{(2)*}$ and $P_{r,n}^*$ are the optimal solution of the inner minimization problem (18) at iteration k , and R_1^* and R_2^* are the corresponding rate values in (15) and (16), respectively. It has been shown

that the subgradient updates in (34) converge to the optimal dual point ν^* as $k \rightarrow \infty$, provided that the step size s_k is chosen according to a diminishing step size rule [34]. The convergence speed of the subgradient method can be improved if one further considers the acceleration techniques in [33], [35], [36]. In Algorithm 1, we summarize the proposed Lagrangian dual optimization algorithm of (P).

C. Simulation Results

In this subsection, we provide some simulation results to examine the performance of the proposed CRN spectrum sharing strategy in (P). The parameters used in the simulations are listed in Table I. Since $N = M = 2$, we simply set $\mathcal{N}_1 = \{1\}$ and $\mathcal{N}_2 = \{2\}$.

We compare the proposed CRN spectrum sharing strategy with two degenerated strategies, namely, the *relay-free* strategy and the *sensing-free* strategy. Similar to the work in [19], the relay-free strategy only considers the direct uplink transmission from the source to the destination. To implement this strategy, we simply set $g_n^{s,r} = g_n^{r,d} = 0$ for Problem (P).

In the sensing-free strategy, the average traffic collision time in (6) becomes

$$\hat{I} = \sum_{m=1}^M \left[\int_{\bigcup_{n \in \mathcal{N}_m} \mathbb{I}_n^{(1)}} \Pr\{X_m(t)=1\} dt + \int_{\bigcup_{n \in \mathcal{N}_m} \mathbb{I}_n^{(2)}} \Pr\{X_m(t)=1\} dt \right], \quad (36)$$

due to the lack of sensing result $X_m(0) = x_m$. It further reduces to

$$\frac{\hat{I}}{T_f} = \sum_{m=1}^M \frac{\lambda_m}{\lambda_m + \mu_m} \left(\hat{\theta}_m^{(1)} + \hat{\theta}_m^{(2)} \right), \quad (37)$$

by means of the interference alignment principle in Lemma 1. Then, the sensing-free strategy is obtained by solving (17) with the objective function in (17a) replaced by (37).

Figure 4(a) presents the performance comparison results of normalized average collision time (I/T_f) versus required uplink spectrum efficiency $R_{\min}/(NW)$. We observe from this figure that for $R_{\min}/(NW) < 0.07$ bits/s/Hz, the relay-free strategy exhibits comparable performance with the proposed strategy; whereas for $R_{\min}/(NW) \geq 0.07$ bits/s/Hz, the proposed strategy yields a smaller average traffic collision time. The performance improvement is attributed to the DF relay techniques. The sensing-free strategy always generates more traffic collisions than the proposed strategy, because it does not utilize the spectrum sensing outcomes.

Figure 4(b) displays the optimal transmission time fractions $\{\theta_n^{(1)}, \theta_n^{(2)}\}_{n=1}^N$ of (P) versus required uplink spectrum efficiency $R_{\min}/(NW)$. The CRN only transmits over sub-channel 1 when $R_{\min}/(NW) \leq 0.42$ bits/s/Hz, because the spectrum sensing outcome indicates that sub-channel 1 is not used by ad-hoc links ($x_1 = 0$) and sub-channel 2 is occupied by ad-hoc links ($x_2 = 1$). For $R_{\min}/(NW) > 0.42$

TABLE I. Parameter setting for Fig. 4.

Parameter	N	M	$\lambda_m T_f$	$\mu_m T_f$	P_{\max}^s	P_{\max}^r	α	δ
Value	2	2	1	1	1	1	0.5	0.1
Parameter	x_1	x_2	$g_1^{s,d}$	$g_1^{s,r}$	$g_1^{r,d}$	$g_2^{s,d}$	$g_2^{s,r}$	$g_2^{r,d}$
Value	0	1	0.4	1.3	1.3	0.5	1.4	1.4

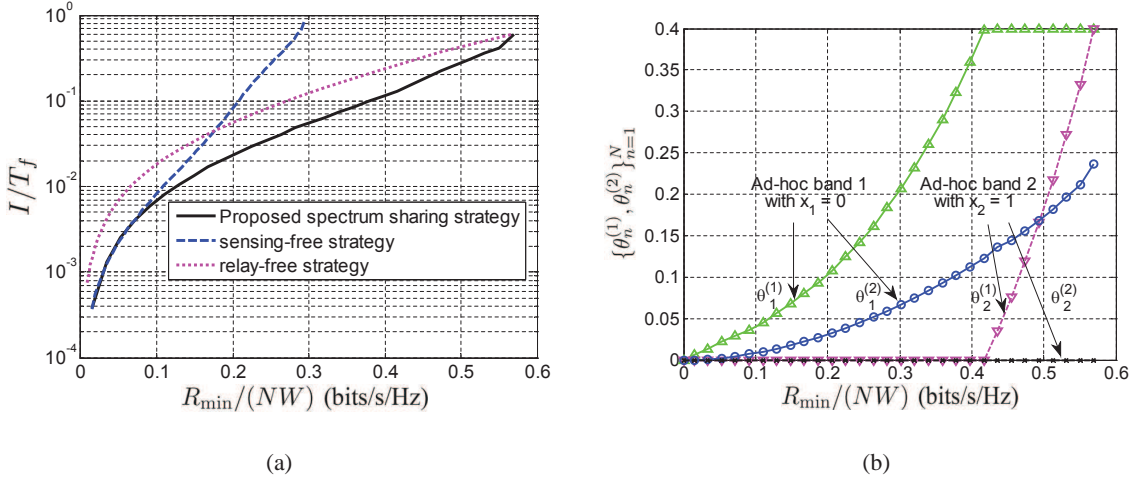


Fig. 4. Simulation results of the proposed frame-level transmission control strategy of the CRN with parameters given in Table I. (a) Normalized average collision time (I/T_f) versus required uplink spectrum efficiency $R_{\min}/(NW)$, (b) optimized transmission time fractions $\{\theta_n^{(1)}, \theta_n^{(2)}\}_{n=1}^N$ versus required uplink spectrum efficiency $R_{\min}/(NW)$.

bits/s/Hz, the CRN starts to transmit over both sub-channels in order to meet the more stringent throughput requirement. The maximal value of $\theta_n^{(1)}$ is $\alpha - \delta = 0.4$, because the computation and signaling delay is $\delta T_f = 0.1 T_f$. On the other hand, it is interesting that $\theta_n^{(2)}$ never achieves the value of $\alpha = 0.5$, even for the largest feasible $R_{\min}/(NW)$. This is because the transmission time $\theta_n^{(2)}$ in Phase 2 only contributes to R_2 , but not to R_1 . When R_1 achieves its maximal value, i.e. $\theta_1^{(1)} = \theta_2^{(1)} = 0.4$, the CRN cannot further increase $R_{CRN} = \min\{R_1, R_2\}$ any more by increasing $\theta_n^{(2)}$.

IV. ERGODIC TRANSMISSION CONTROL AND REAL-TIME IMPLEMENTATION

In the previous section, the optimal transmission control solution is computed for each frame. As we mentioned in Section I, such a frame-level spectrum sharing strategy may encounter several implementation issues. The CRN has to solve the optimal transmission Problem (P) for every frame, which may be computationally too demanding for realistic wireless communication systems. Moreover, the destination

node has to collect the spectrum sensing outcome from the source and/or relay nodes in order to solve (P). After solving (P), the destination node has to send the solutions back to the source and relay nodes. The information signaling and solution computation process may cause a considerable control delay δT_f , leaving very short time for data transmission.

These issues intrigue us to investigate more practical spectrum sharing strategies that allow real-time implementations. The key ideas are 1) to reduce the amount of real-time computations and 2) to decrease the control delay between spectrum sensing and data transmission. Our approach is to consider an *ergodic* resource allocation problem. Recall from Section III-A that the frame-level design problem (17) can be solved by the Lagrangian dual optimization method in Algorithm 1. We will show next that for the ergodic resource allocation problem, one can compute the optimal dual variable ν^* off-line, and only some simple tasks are left for real-time computation.

After obtaining ν^* , we need to compute the transmission parameters based on real-time spectrum sensing and channel estimation results. These real-time computation tasks are carefully assigned to the relay and source nodes in order to minimize the computation and signaling delay δT_f .

Another benefit of this ergodic setting is that it allows one more spectrum sensing at the beginning of Phase 2 to improve the performance of collision mitigation. This, however, cannot be exploited in the frame-level setting, because Problem (P) must be solved before this additional sensing outcome is obtained.

A. Ergodic Transmission Control and Its Practical Implementations

Suppose that both of the source and relay nodes perform one extra spectrum sensing at the beginning of Phase 2. The sensing outcome for the m th ad-hoc band is denoted as $X_m(\alpha T_f) = y_m \in \{0, 1\}$ with $m = 1, \dots, M$. This additional sensing outcome can be included in the resource allocation problem to reduce traffic collision, which leads to an extra computation and signaling delay in Phase 2, as shown in Fig. 5. For the ease of expression, the duration of this extra computation and signaling delay is also assumed to be δT_f .

Let us define a network state information (NSI) as

$$\omega \triangleq \{g_n^{s,d}, g_n^{s,r}, g_n^{r,d}, x_m, y_m, n \in \mathcal{N}, m \in \mathcal{M}\},$$

which includes both the channel estimation and spectrum sensing results over the two phases. In the ergodic transmission control problem, the NSI ω varies across frames. We assume that the channel fading gains and the ad-hoc traffic are stationary and ergodic; furthermore, their statistical distributions are known to the destination.

Similar to (6), the average traffic collision time for a frame with NSI ω is determined by

$$I(\omega) = \sum_{m=1}^M \left(\int_{\bigcup_{n \in \mathcal{N}_m} \mathbb{I}_n^{(1)}(\omega)} \Pr\{X_m(t)=1|X_m(0)=x_m\}dt + \int_{\bigcup_{n \in \mathcal{N}_m} \mathbb{I}_n^{(2)}(\omega)} \Pr\{X_m(t)=1|X_m(\alpha T_f)=y_m\}dt \right), \quad (38)$$

where $\mathbb{I}_n^{(i)}(\omega)$ denotes the set of CRN transmission time over sub-channel n in phase i given the NSI ω . Note from (38) that, in contrast to (6), the collision time in Phase 2 now depends on the sensing outcome y_m . Since the NSI is stationary and ergodic across the frames, the long term average traffic collision time can be obtained by taking the expectation of $I(\omega)$ over the distribution of the NSI ω [25], i.e.,

$$\bar{I} = \mathbb{E}_{\omega} \left[\sum_{m=1}^M \left(\int_{\bigcup_{n \in \mathcal{N}_m} \mathbb{I}_n^{(1)}(\omega)} \Pr\{X_m(t)=1|X_m(0)=x_m\}dt + \int_{\bigcup_{n \in \mathcal{N}_m} \mathbb{I}_n^{(2)}(\omega)} \Pr\{X_m(t)=1|X_m(\alpha T_f)=y_m\}dt \right) \right]. \quad (39)$$

Let us define the transmission time fractions $\theta_n^{(i)}(\omega)$ as in (1), and define

$$\hat{\theta}_m^{(i)}(\omega) \triangleq \max \left\{ \theta_n^{(i)}(\omega), n \in \mathcal{N}_m \right\}, \quad (40)$$

for $m = 1, \dots, M$ and $i = 1, 2$. It is not difficult to show that the optimal spectrum access strategies stated in Lemma 1 also hold true for the case with two spectrum sensings in each frame:

Lemma 2 *For any given transmission time fractions $\{\hat{\theta}_m^{(1)}(\omega) \in [0, \alpha - \delta], \hat{\theta}_m^{(2)}(\omega) \in [0, 1 - \alpha - \delta]\}_{m=1}^M$ we have that:*

- 1) *The optimal spectrum access strategy of Phase 1 is given by $\mathbb{I}_n^{(1)}(\omega) = [\delta T_f, (\delta + \hat{\theta}_m^{(1)}(\omega))T_f]$ ($\mathbb{I}_n^{(1)}(\omega) = [(\alpha - \hat{\theta}_m^{(1)}(\omega))T_f, \alpha T_f]$) for all $n \in \mathcal{N}_m$, if the sensing outcome of Phase 1 is $x_m = 0$ ($x_m = 1$);*
- 2) *The optimal spectrum access strategy of Phase 2 is given by $\mathbb{I}_n^{(2)}(\omega) = [(\alpha + \delta)T_f, (\alpha + \delta + \hat{\theta}_m^{(2)}(\omega))T_f]$ ($\mathbb{I}_n^{(2)}(\omega) = [(1 - \hat{\theta}_m^{(2)}(\omega))T_f, T_f]$) for all $n \in \mathcal{N}_m$, if the sensing outcome of Phase 2 is $y_m = 0$ ($y_m = 1$).*

An example of Lemma 2 is illustrated in Fig. 5. Define the two functions

$$\begin{aligned} \hat{\phi}_{(2)}(\theta; y_m = 0) &= \int_{[(\alpha + \delta)T_f, (\theta + \alpha + \delta)T_f]} \Pr(X_m(t)=1|X_m(\alpha T_f) = 0)dt \\ &= \frac{\lambda_m}{\lambda_m + \mu_m} \left\{ \theta + \frac{1}{(\lambda_m + \mu_m)T_f} e^{-(\lambda_m + \mu_m)\delta T_f} \left[e^{-(\lambda_m + \mu_m)\theta T_f} - 1 \right] \right\} T_f, \end{aligned} \quad (41)$$

$$\begin{aligned} \hat{\phi}_{(2)}(\theta; y_m = 1) &= \int_{[T_f - \theta T_f, T_f]} \Pr(X_m(t) = 1|X_m(\alpha T_f) = 1)dt \\ &= \frac{\lambda_m}{\lambda_m + \mu_m} \left\{ \theta + \frac{\mu_m}{\lambda_m} \frac{1}{(\lambda_m + \mu_m)T_f} e^{-(\lambda_m + \mu_m)(1 - \alpha)T_f} \left[e^{(\lambda_m + \mu_m)\theta T_f} - 1 \right] \right\} T_f, \end{aligned} \quad (42)$$

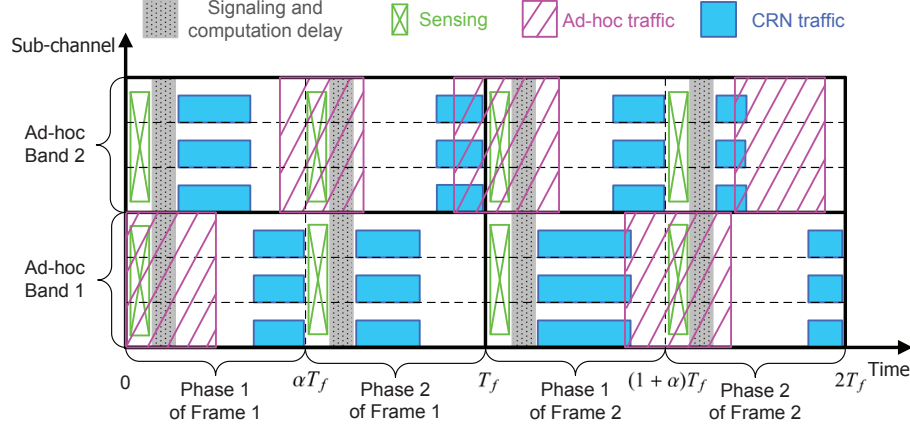


Fig. 5. Time-frequency transmission structure by Lemma 2. Here the sensing outcomes of frame 1 are $x_1 = 1$, $x_2 = 0$, $y_1 = 0$ and $y_2 = 0$, and the the sensing outcomes of frame 2 are $x_1 = 0$, $x_2 = 1$, $y_1 = 1$ and $y_2 = 0$.

where $\theta \in [0, 1 - \alpha]$. In accordance with Lemma 2, \bar{I} in (39) can be simplified as

$$\bar{I} = \mathbb{E}_{\omega} \left\{ \sum_{m=1}^M \left[\phi_{(1)} \left(\hat{\theta}_m^{(1)}(\omega); x_m \right) + \hat{\phi}_{(2)} \left(\hat{\theta}_m^{(2)}(\omega); y_m \right) \right] \right\}, \quad (43)$$

where $\phi_{(1)}(\theta, x_m)$ has been defined in (9) and (10) for $x_m = 0$ and $x_m = 1$, respectively.

The achievable average rate of the multi-carrier CRN can be shown to be

$$\bar{R}_{CRN} = \min \{ \bar{R}_1, \bar{R}_2 \}, \quad (44)$$

where

$$\bar{R}_1 = W \sum_{m \in \mathcal{M}} \sum_{n \in \mathcal{N}_m} \mathbb{E}_{\omega} \left[\hat{\theta}_m^{(1)}(\omega) \log_2 \left(1 + \frac{P_{s,n}^{(1)}(\omega) \max\{g_n^{s,r}, g_n^{s,d}\}}{\hat{\theta}_m^{(1)}(\omega)} \right) + \hat{\theta}_m^{(2)}(\omega) \log_2 \left(1 + \frac{P_{s,n}^{(2)}(\omega) g_n^{s,d}}{\hat{\theta}_m^{(2)}(\omega)} \right) \right], \quad (45)$$

$$\bar{R}_2 = W \sum_{m \in \mathcal{M}} \sum_{n \in \mathcal{N}_m} \mathbb{E}_{\omega} \left[\hat{\theta}_m^{(1)}(\omega) \log_2 \left(1 + \frac{P_{s,n}^{(1)}(\omega) g_n^{s,d}}{\hat{\theta}_m^{(1)}(\omega)} \right) + \hat{\theta}_m^{(2)}(\omega) \log_2 \left(1 + \frac{P_{s,n}^{(2)}(\omega) g_n^{s,d} + P_{r,n}(\omega) g_n^{r,d}}{\hat{\theta}_m^{(2)}(\omega)} \right) \right], \quad (46)$$

and $P_{s,n}^{(1)}(\omega)$, $P_{s,n}^{(2)}(\omega)$, $P_{r,n}(\omega)$ are the transmission powers for a given NSI ω . We should point out that the average rate \bar{R}_{CRN} is not the ergodic data rate in the Shannon sense, but one achieved by taking the average over many adaptive channel coding blocks. The relay node will not transmit but queue up its received data from the source node [21], [37], until the channel quality and sensing outcome in Phase 2 is favorable.

It follows from (43) and (44) that the ergodic spectrum access and resource allocation problem is

$$\min_{\substack{P_{s,n}^{(1)}(\omega), P_{s,n}^{(2)}(\omega), P_{r,n}(\omega), \hat{\theta}_m^{(1)}(\omega), \hat{\theta}_m^{(2)}(\omega), \\ n=1, \dots, N, m=1, \dots, M}} \mathbb{E}_{\omega} \left\{ \sum_{m=1}^M \left[\phi_{(1)} \left(\hat{\theta}_m^{(1)}(\omega); x_m \right) + \hat{\phi}_{(2)} \left(\hat{\theta}_m^{(2)}(\omega); y_m \right) \right] \right\} \quad (47a)$$

$$\text{s.t.} \quad \bar{R}_1 \geq \bar{R}_{\min}, \quad \bar{R}_2 \geq \bar{R}_{\min} \quad (47b)$$

$$\mathbb{E}_{\omega} \left\{ \sum_{n=1}^N \left[P_{s,n}^{(1)}(\omega) + P_{s,n}^{(2)}(\omega) \right] \right\} \leq \bar{P}_{\max}^s \quad (47c)$$

$$\mathbb{E}_{\omega} \left\{ \sum_{n=1}^N P_{r,n}(\omega) \right\} \leq \bar{P}_{\max}^r \quad (47d)$$

$$P_{s,n}^{(1)}(\omega), P_{s,n}^{(2)}(\omega), P_{r,n}(\omega) \geq 0, \quad n = 1, \dots, N \quad (47e)$$

$$0 \leq \hat{\theta}_m^{(1)}(\omega) \leq \alpha - \delta, 0 \leq \hat{\theta}_m^{(2)}(\omega) \leq 1 - \alpha - \delta, \quad m = 1, \dots, M. \quad (47f)$$

B. Lagrangian Optimization Method for Problem (47)

In the sequel, we provide the implementation method to solve Problem (47) following the idea in Section III-B. Specifically, we solve the following dual optimization problem

$$\max_{\zeta, \sigma, \varepsilon, \eta \geq 0} \left(\min_{(P_{s,n}^{(1)}(\omega), P_{s,n}^{(2)}(\omega), P_{r,n}(\omega), \hat{\theta}_m^{(1)}(\omega), \hat{\theta}_m^{(2)}(\omega)) \in \bar{\mathcal{V}}} \bar{L} \right) \quad (48)$$

where $\bar{\mathcal{V}} \triangleq \left\{ \left(P_{s,n}^{(1)}(\omega), P_{s,n}^{(2)}(\omega), P_{r,n}(\omega), \hat{\theta}_m^{(1)}(\omega), \hat{\theta}_m^{(2)}(\omega) \right) \mid 0 \leq \hat{\theta}_m^{(1)}(\omega) \leq \alpha - \delta, 0 \leq \hat{\theta}_m^{(2)}(\omega) \leq 1 - \alpha - \delta, P_{s,n}^{(1)}(\omega), P_{s,n}^{(2)}(\omega), P_{r,n}(\omega) \geq 0, n \in \mathcal{N}, m \in \mathcal{M} \right\}$, and

$$\begin{aligned} \bar{L} = & \frac{1}{T_f} \mathbb{E}_{\omega} \left\{ \sum_{m=1}^M \left[\phi_{(1)} \left(\hat{\theta}_m^{(1)}(\omega); x_m \right) + \hat{\phi}_{(2)} \left(\hat{\theta}_m^{(2)}(\omega); y_m \right) \right] \right\} + \frac{\zeta}{W} (\bar{R}_{\min} - \bar{R}_1) + \frac{\sigma}{W} (\bar{R}_{\min} - \bar{R}_2) \\ & + \varepsilon \left\{ \mathbb{E}_{\omega} \left\{ \sum_{n=1}^N \left[P_{s,n}^{(1)}(\omega) + P_{s,n}^{(2)}(\omega) \right] \right\} - \bar{P}_{\max}^s \right\} + \eta \left\{ \mathbb{E}_{\omega} \left[\sum_{n=1}^N P_{r,n}(\omega) \right] - \bar{P}_{\max}^r \right\}, \end{aligned} \quad (49)$$

is the partial Lagrangian of (47).

Let us define $\omega_{\ell} \triangleq \{g_n^{s,r}(\ell), g_n^{s,d}(\ell), g_n^{r,d}(\ell), x_m(\ell), y_m(\ell), n \in \mathcal{N}, m \in \mathcal{M}\}$ as the NSI of the ℓ th frame. Problem (48) is in general non-causal, because it requires the NSI realizations $\{\omega_{\ell}\}_{\ell=1}^{\infty}$ of future frames to solve the inner minimization problem. However, by making use of the statistical distribution of the NSI, we can solve Problem (48) in two steps: First, we optimize the dual variables $\nu = (\zeta, \sigma, \varepsilon, \eta)^T$ *off-line* based on only the statistical distribution of the NSI. Then, the primal solution is updated *on-line* according to the current NSI ω_{ℓ} . Most computation tasks are accomplished in the off-line dual optimization step, leaving only simple computations for real-time primal solution update, as we detail in the subsequent two subsections.

C. Off-line Dual Optimization

Given a dual variable $\boldsymbol{\nu} = (\zeta, \varphi, \varepsilon, \eta)^T$, the optimal solution to the inner minimization problem of (48) for the NSI realization $\boldsymbol{\omega}$ is provided as follows:

The optimal $\frac{P_{s,n}^{(1)}(\boldsymbol{\omega})}{\hat{\theta}_m^{(1)}(\boldsymbol{\omega})}$, $\frac{P_{s,n}^{(2)}(\boldsymbol{\omega})}{\hat{\theta}_m^{(2)}(\boldsymbol{\omega})}$ and $\frac{P_{r,n}(\boldsymbol{\omega})}{\hat{\theta}_m^{(1)}(\boldsymbol{\omega})}$ of the inner minimization problem of (48) can be exactly obtained by (25)-(29), with $P_{s,n}^{(i)}$, $P_{r,n}$ and $\hat{\theta}_m^{(i)}$ replaced by $P_{s,n}^{(i)}(\boldsymbol{\omega})$, $P_{r,n}(\boldsymbol{\omega})$ and $\hat{\theta}_m^{(i)}(\boldsymbol{\omega})$, respectively. The optimal $\hat{\theta}_m^{(1)}(\boldsymbol{\omega})$ can be obtained by either (30) or (32), depending on the sensing result x_m . By (41) and (42), the optimal $\hat{\theta}_m^{(2)}(\boldsymbol{\omega})$ is given as follows: If $y_m = 0$,

$$\hat{\theta}_m^{(2)}(\boldsymbol{\omega}) = \min \left\{ \left[-\frac{1}{(\lambda_m + \mu_m)T_f} \ln \left\{ 1 - \frac{\lambda_m + \mu_m}{\lambda_m} \sum_{n \in \mathcal{N}_m} \left[\zeta f \left(g_n^{s,d} \frac{P_{s,n}^{(2)}(\boldsymbol{\omega})}{\hat{\theta}_m^{(2)}(\boldsymbol{\omega})} \right) + \sigma f \left(g_n^{s,d} \frac{P_{s,n}^{(2)}(\boldsymbol{\omega})}{\hat{\theta}_m^{(2)}(\boldsymbol{\omega})} + g_n^{r,d} \frac{P_{r,n}(\boldsymbol{\omega})}{\hat{\theta}_m^{(2)}(\boldsymbol{\omega})} \right) \right] \right\} - \delta \right]^+, 1 - \alpha - \delta \right\}; \quad (50)$$

otherwise,

$$\hat{\theta}_m^{(2)}(\boldsymbol{\omega}) = \min \left\{ \left[1 - \alpha + \frac{1}{(\lambda_m + \mu_m)T_f} \ln \left\{ \frac{\lambda_m + \mu_m}{\mu_m} \sum_{n \in \mathcal{N}_m} \left[\zeta f \left(g_n^{s,d} \frac{P_{s,n}^{(2)}(\boldsymbol{\omega})}{\hat{\theta}_m^{(2)}(\boldsymbol{\omega})} \right) + \sigma f \left(g_n^{s,d} \frac{P_{s,n}^{(2)}(\boldsymbol{\omega})}{\hat{\theta}_m^{(2)}(\boldsymbol{\omega})} + g_n^{r,d} \frac{P_{r,n}(\boldsymbol{\omega})}{\hat{\theta}_m^{(2)}(\boldsymbol{\omega})} \right) \right] - \frac{\lambda_m}{\mu_m} \right\} \right]^+, 1 - \alpha - \delta \right\}. \quad (51)$$

By substituting (30), (32), (50) and (51) into (25)-(29), the optimal values of $P_{s,n}^{(1)}(\boldsymbol{\omega})$, $P_{s,n}^{(2)}(\boldsymbol{\omega})$ and $P_{r,n}(\boldsymbol{\omega})$ can then be obtained.

The optimal dual variable $\boldsymbol{\nu}^*$ is obtained by a series of the subgradient update in (34), where the subgradient $\mathbf{h}(\boldsymbol{\nu}_k)$ is determined by

$$\mathbf{h}(\boldsymbol{\nu}_k) = \begin{bmatrix} (\bar{R}_{\min} - \bar{R}_1^*)/W \\ (\bar{R}_{\min} - \bar{R}_2^*)/W \\ \sum_{n=1}^N \mathbb{E}_{\boldsymbol{\omega}} \left\{ P_{s,n}^{(1)*}(\boldsymbol{\omega}) + P_{s,n}^{(2)*}(\boldsymbol{\omega}) \right\} - \bar{P}_{\max}^s \\ \sum_{n=1}^N \mathbb{E}_{\boldsymbol{\omega}} \left\{ P_{r,n}^*(\boldsymbol{\omega}) \right\} - \bar{P}_{\max}^r \end{bmatrix}, \quad (52)$$

where $P_{s,n}^{(1)*}(\boldsymbol{\omega})$, $P_{s,n}^{(2)*}(\boldsymbol{\omega})$ and $P_{r,n}^*(\boldsymbol{\omega})$ are the optimal solution of the inner minimization problem (48) for given dual variable $\boldsymbol{\nu}_k$ and NSI realization $\boldsymbol{\omega}$, and \bar{R}_1^* and \bar{R}_2^* are the corresponding rate values in (45) and (46), respectively. Although the true NSI realizations $\{\boldsymbol{\omega}_\ell\}_{\ell=1}^\infty$ are not available, we can still compute the expectation terms in (45), (46) and (52) by Monte Carlo simulations. In particular, one may randomly generate a set of NSI realizations $\boldsymbol{\omega}$ following the distribution of the channel fading and sensing outcome. Then, the inner minimization problem of (48) is solved for each artificially generated NSI realization $\boldsymbol{\omega}$. The expectation terms in (45), (46) and (52) can be obtained by averaging over these NSI realizations.

D. On-line Primal Solution Update

After ν^* is obtained, one can compute the optimal transmission parameters of Problem (47) based on the true NSI $\{\omega_\ell\}_{\ell=1}^\infty$. More specifically, in frame ℓ , the CRN needs to solve the inner minimization problem of (48) for the optimal dual variable $\nu = \nu^*$ and NSI sample $\omega = \omega_\ell$. The computation complexity of this step is much smaller than that of off-line dual optimization, because each iteration of dual variable update involves solving one inner minimization problem of (48) for a set of NSI realizations. On the other hand, spectrum sensing and channel estimation are usually performed at spatially separated nodes, and thus additional information exchanges are required to accomplish the computation task.

In the sequel, we present how to update real-time primal solution such that the computation and signaling delay δT_f can be substantially decreased. In practice, the BS is able to acquire the channel gain $\{g_n^{s,r}(\ell), g_n^{s,d}(\ell), g_n^{r,d}(\ell)\}_{n=1}^N$ through channel prediction before frame ℓ , if the wireless channel varies slowly across the frames [38]. Given the channel gain $\{g_n^{s,r}(\ell), g_n^{s,d}(\ell), g_n^{r,d}(\ell)\}$, the BS can compute the ratios $\frac{P_{s,n}^{(1)}(\omega_\ell)}{\hat{\theta}_m^{(1)}(\omega_\ell)}$, $\frac{P_{s,n}^{(2)}(\omega_\ell)}{\hat{\theta}_m^{(2)}(\omega_\ell)}$ and $\frac{P_{r,n}(\omega_\ell)}{\hat{\theta}_m^{(2)}(\omega_\ell)}$ according to (25)-(29) in frame $\ell - 1$, and then feed the results back to the source and relay nodes before the beginning of frame ℓ . Once the source and relay nodes obtain the sensing outcomes $x_m(\ell)$ and $y_m(\ell)$, they can compute $\hat{\theta}_m^{(1)}(\omega_\ell)$ and $\hat{\theta}_m^{(2)}(\omega_\ell)$ according to (30), (32), (50), and (51). By providing the source and relay nodes with $\frac{P_{s,n}^{(1)}(\omega_\ell)}{\hat{\theta}_m^{(1)}(\omega_\ell)}$, $\frac{P_{s,n}^{(2)}(\omega_\ell)}{\hat{\theta}_m^{(2)}(\omega_\ell)}$ and $\frac{P_{r,n}(\omega_\ell)}{\hat{\theta}_m^{(2)}(\omega_\ell)}$ ahead of time, the signaling procedure will not cause additional control delay. As $\hat{\theta}_m^{(1)}(\omega_\ell)$ and $\hat{\theta}_m^{(2)}(\omega_\ell)$ can be computed with the previously presented closed-form expressions, the resulting computation delay δT_f is quite short. Note that the signaling overhead of this primal solution computation strategy is equal to that of conventional OFDM CRN without spectrum sharing [21], where the BS also needs to feed the ratios $\frac{P_{s,n}^{(1)}(\omega_\ell)}{\hat{\theta}_m^{(1)}(\omega_\ell)}$, $\frac{P_{s,n}^{(2)}(\omega_\ell)}{\hat{\theta}_m^{(2)}(\omega_\ell)}$ and $\frac{P_{r,n}(\omega_\ell)}{\hat{\theta}_m^{(2)}(\omega_\ell)}$ back to the source and relay nodes.

In practice, the source and relay nodes may not be able to compute $\hat{\theta}_m^{(1)}(\omega_\ell)$ and $\hat{\theta}_m^{(2)}(\omega_\ell)$, owing to hardware limitations. In this case, the BS can compute two possible values of $\hat{\theta}_m^{(1)}(\omega_\ell)$ in (30) and (32) in advance for both $x_m(\ell) = 1$ and $x_m(\ell) = 0$. Similarly, $\hat{\theta}_m^{(2)}(\omega_\ell)$ in (50) and (51) can also be computed in advance at the BS for both $y_m(\ell) = 0$ and $y_m(\ell) = 1$. The BS sends $\frac{P_{s,n}^{(1)}(\omega_\ell)}{\hat{\theta}_m^{(1)}(\omega_\ell)}$, $\frac{P_{s,n}^{(2)}(\omega_\ell)}{\hat{\theta}_m^{(2)}(\omega_\ell)}$ and $\frac{P_{r,n}(\omega_\ell)}{\hat{\theta}_m^{(2)}(\omega_\ell)}$ and the two possible values of $\hat{\theta}_m^{(1)}(\omega_\ell)$ and $\hat{\theta}_m^{(2)}(\omega_\ell)$ to the source and relay nodes. After spectrum sensing, the source and relay nodes simply select the values of $\hat{\theta}_m^{(1)}(\omega_\ell)$ and $\hat{\theta}_m^{(2)}(\omega_\ell)$ according to the sensing outcomes $x_m(\ell)$ and $y_m(\ell)$, respectively. Because of only two possible values of $\hat{\theta}_m^{(i)}(\omega_\ell)$ for the m th ad-hoc band in Phase i , the extra signaling overhead for transmitting $\hat{\theta}_m^{(i)}(\omega_\ell)$ is not too large. This primal solution computation strategy has two benefits: First, all computations are carried out at the BS, and source and relay nodes only need to select appropriate transmission parameters. Second, the source

and relay nodes can start transmission right after spectrum sensing, which means the computation and signaling delay δT_f is negligible.

Remark 2: With the optimal dual solution ν^* obtained ahead of time, the transmission parameters of the CRN in Phase 1 is determined solely by $x_m(\ell)$ but not $y_m(\ell)$. Hence, the primal solution to the ergodic transmission control problem can be computed in a causal manner. However, $y_m(\ell)$ cannot be exploited in the frame-level transmission control problem (P), because neither the dual optimal solution ν^* nor the primal optimal solution to (P) can be obtained in advance without $y_m(\ell)$.

Remark 3: If the source transmits to the relay node in Phase 1, and the sensing outcome of Phase 2 becomes unfavorable, the relay node will queue up its received data from the source node, and wait for better transmission opportunity [21], [37]. Therefore, data queuing at the relay node allow us to handle the transmissions in two phases separately, as long as the average data rate of the source node is no larger than \bar{R}_{CRN} in (44).

Remark 4: In practice, sensing error may occur at the source and relay nodes, which means that the ACTIVE (IDLE) ad-hoc traffic state is mistakenly detected as IDLE (ACTIVE). This will lead to incoordination between the source and relay nodes, and hence unexpected interference to the ad-hoc links. However, the achievable rate of the CRN would not be affected by sensing error, because the source and relay nodes transmit to the destination node in asynchronous fashion, i.e. the destination node first decodes the relay's message, and then decodes the source's message [21]. The performance degradation caused by sensing error is examined in the next subsection.

E. Simulation Results

We present some simulation results in this subsection to demonstrate the effectiveness of the proposed ergodic CRN spectrum sharing strategy in (47). The number of sub-channels is 16 ($N = 16$) and the number of ad-hoc bands is 4 ($M = 4$). Each ad-hoc band overlaps with 4 consecutive CRN sub-channels, and the 4 ad-hoc bands do not overlap with each other. α is set to 0.5.

The channel coefficients $h_n^{i,j}$ (where $i \in \{s, r\}$ and $j \in \{r, d\}$, $i \neq j$) are modeled as independent and identically distributed Rayleigh fading with zero mean and unit variance. We assume that the relay is located right in the middle of the source and the destination. The large-scale path loss factor of all the wireless links is set to 4. Suppose that the signal-to-interference-plus-noise ratio (SINR) of the source-destination link is set to $\frac{P_{\max}^s \mathbb{E}\{|h_n^{s,d}|^2\}}{NWN_n^d} = 5\text{dB}$. Assuming that $N_n^r = N_n^d$ and $P_{\max}^s = P_{\max}^r$, both the SINRs of the source-relay and relay-destination links are equal to $\frac{P_{\max}^s \mathbb{E}\{|h_n^{s,r}|^2\}}{NWN_n^r} = \frac{P_{\max}^r \mathbb{E}\{|h_n^{r,d}|^2\}}{NWN_n^d} = 17\text{dB}$ based on the path-loss factor. The simulation results are obtained by averaging over 500 realizations of

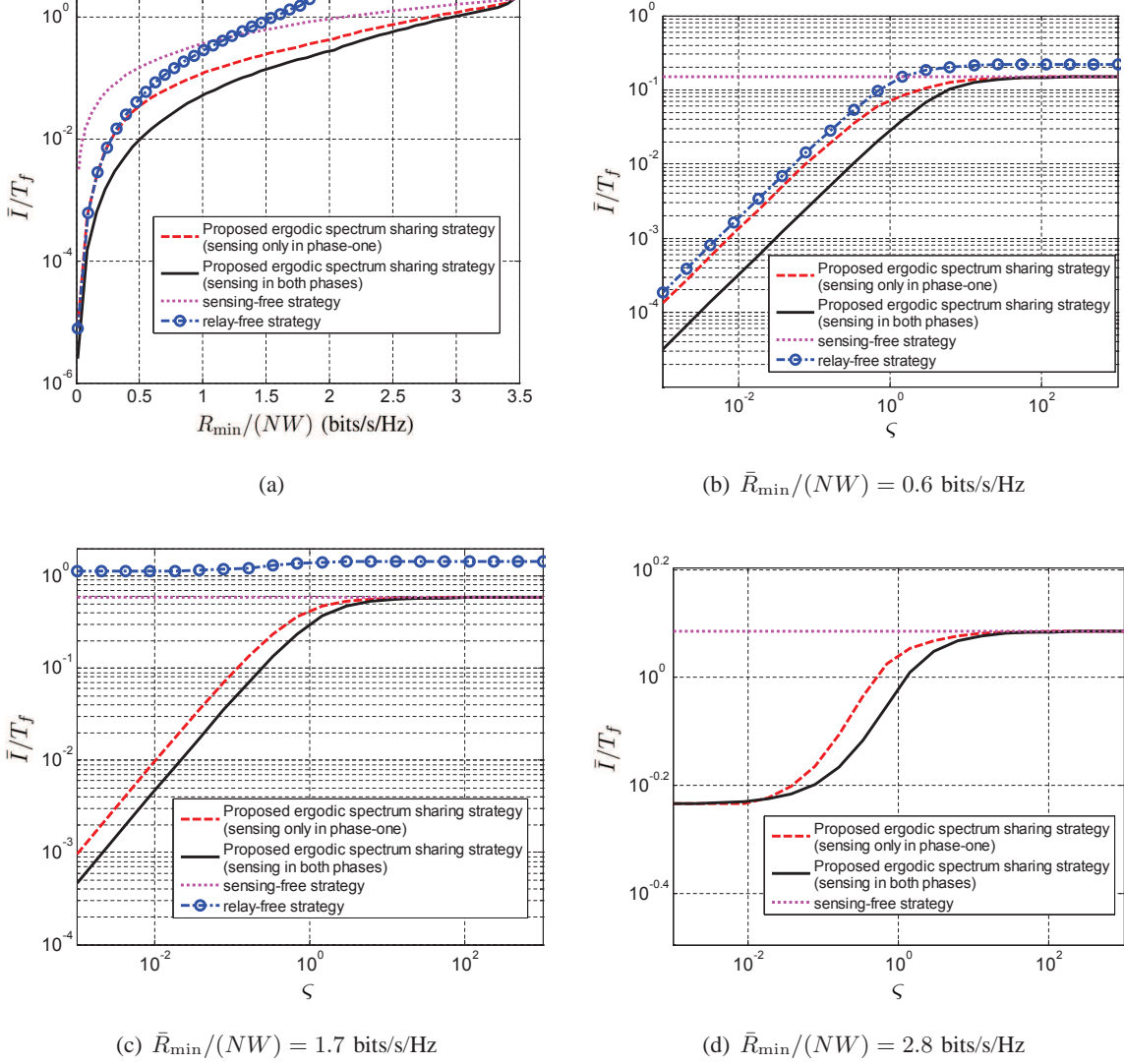


Fig. 6. Simulation results of the proposed ergodic transmission control strategy of the CRN. (a) Normalized long term average collision time (\bar{I}/T_f) versus required long term average uplink spectrum efficiency $\bar{R}_{\min}/(NW)$, (b)-(d) \bar{I}/T_f versus ζ for $\lambda = \mu$ and various values of $\bar{R}_{\min}/(NW)$.

NSI (averaging over 500 frames). In our real-time implementation method, the computation and signaling delay is negligible, which means we can choose $\delta = 0$.

Figure 6(a) shows the simulation results of normalized long term average collision time (\bar{I}/T_f) versus required long term average uplink spectrum efficiency $\bar{R}_{\min}/(NW)$, for $\lambda_m T_f = \mu_m T_f = 1$ for all $m = 1, \dots, M$. To compare with the proposed ergodic CRN spectrum sharing strategy, we also perform the same simulations with its relay-free and sensing-free counterparts. The performance of the proposed CRN strategy using only phase-1 spectrum sensing is also presented. We can observe from Fig. 6(a) that

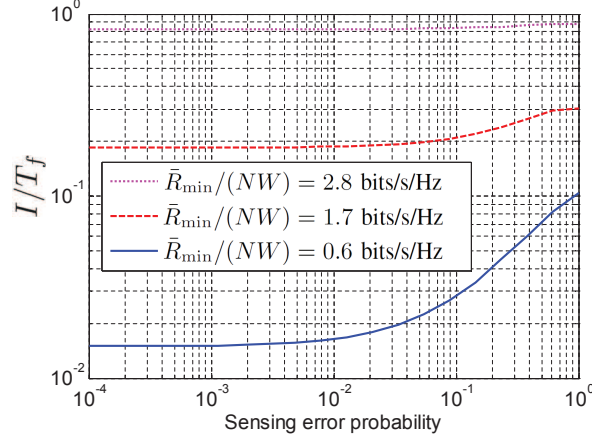


Fig. 7. Simulation results of normalized long term average collision time (\bar{I}/T_f) versus sensing error probability, for different values of $\bar{R}_{\min}/(NW)$.

the proposed strategy outperforms both the relay-free strategy and the sensing-free strategy. Moreover, the proposed strategy with spectrum sensing in two phases performs better than with only phase-1 spectrum sensing.

To further examine how the behavior of the ad-hoc traffic affects the performance of the proposed strategy, we define a parameter, called *the relative variation rate of the ad-hoc traffic state* or *the relative sensing period of the CRN*, as

$$\varsigma \triangleq \frac{T_f}{\frac{1}{\lambda} + \frac{1}{\mu}}, \quad (53)$$

where $\lambda = \lambda_m$ and $\mu = \mu_m$ for all m . A small value of ς (that corresponds to small values of λ and μ) implies that the on-off state of the ad-hoc traffic changes slowly in each CRN frame. However, the ad-hoc traffic state would change many times in each CRN frame if ς is large (that corresponds to large values of λ and μ). Figures 6(b) to 6(d) show the simulation results of normalized average collision time (\bar{I}/T_f) versus relative variation rate ς for $\lambda = \mu$ and various values of $\bar{R}_{\min}/(NW)$. From Fig. 6(b), one can observe that the proposed strategy performs best. However, the performance gaps between the proposed strategy and the relay-free and sensing-free strategies decrease with ς , because the ad-hoc traffic is more difficult to predict for large ς . For very large values of ς , the proposed strategy has similar performance with the sensing-free strategy. Therefore, spectrum sensing provides no further benefit in this case.

We can also see from Fig. 6(b) and Fig. 6(c) that the performance of the relay-free strategy seriously degrades as $\bar{R}_{\min}/(NW)$ increases from 0.6 bits/s/Hz to 1.7 bits/s/Hz. The performance degradation of the relay-free strategy is much larger than that of the proposed strategy because the CRN is capable of

supporting higher uplink throughput than the relay-free strategy. In Fig. 6(d), the results of the relay-free strategy are not shown because this strategy is not feasible in supporting $\bar{R}_{\min}/(NW) = 2.8$ bits/s/Hz.

We finally examine the robustness of our proposed strategy against sensing error. Figure 7 shows the simulation results of normalized long term average collision time (\bar{I}/T_f) versus sensing error probability, for different values of $\bar{R}_{\min}/(NW)$. One can observe from Fig. 7 that, if the sensing error probability is small, e.g. less than 0.01, the performance degradation of our proposed strategy is insignificant.

V. CONCLUDING REMARKS

In this paper, we have investigated optimal transmission control for spectrum sharing between cooperative relay and ad-hoc networks. Physical-layer resource allocation and MAC-layer spectrum access of the CRN are jointly optimized such that the average traffic collision time between the two networks is minimized while guaranteeing the CRN throughput requirement. Both frame-level design and ergodic design are presented. For the latter design, a real-time implementation method of the optimal transmission control strategy has been proposed, by exploiting the structure of Lagrangian dual optimization solution. This implementation method has the following benefits:

- 1) Most computations are accomplished off-line, leaving only simple tasks for real-time computations.
- 2) Although the sensing outcomes and channel gains are collected at spatially separate nodes, the information exchange does not cause additional control delay.
- 3) The computations at the source and relay nodes can be avoided, at a cost of insignificant signaling overhead.
- 4) Additional spectrum sensing in Phase 2 can be exploited to improve collision prediction. The relay node can queue up its received data if the sensing outcome in Phase 2 is unfavorable, which provides more freedom for collision mitigation.

Simulation results have been provided to examine the performance of the proposed strategy. We have found that good collision mitigation performance can be achieved if the ad-hoc traffic varies slowly and the required throughput of the relay network is not too high. The presented implementation techniques may be useful for optimal real-time control of other wireless communication systems.

We have assumed that the channel coefficients remain static within each frame and is perfectly known to the BS. In practice, imperfect channel state information may occur due to time-varying nature of the channel, or limitations of the estimation technique and feedback channel [39]. In this case, compound achievable rate of OFDM DF relaying, which can be simply obtained based on the results of [39], can be

adopted in the optimization problem to provide a robust transmission strategy for any channel uncertainty in a bounded region.

Our studies are based on the CTMC model for the ad-hoc traffic. Devising optimal spectrum sharing strategies based on models that fit practical ad-hoc traffic better than the CTMC model (e.g., the semi-Markov model [9]) is of great interest and is currently under our investigation.

ACKNOWLEDGEMENTS

The authors would like to thank P. R. Kumar, Lang Tong, Yongle Wu, Ying Cui and Ness B. Shroff for constructive discussions about this work.

APPENDIX A

PROOF OF Lemma 1

For $i \in \{1, 2\}$, suppose that $\theta_{n'}^{(i)} = \hat{\theta}_m^{(i)}$ for some $n' \in \mathcal{N}_m$, i.e., sub-channel n' has the longest transmission time among the sub-channels in \mathcal{N}_m . Because $\mathbb{I}_{n'}^{(i)} \subseteq \bigcup_{n \in \mathcal{N}_m} \mathbb{I}_n^{(i)}$, we have

$$\int_{\mathbb{I}_{n'}^{(i)}} \Pr \{X_m(t) = 1 | X_m(0) = x_m\} dt \leq \int_{\bigcup_{n \in \mathcal{N}_m} \mathbb{I}_n^{(i)}} \Pr \{X_m(t) = 1 | X_m(0) = x_m\} dt. \quad (1)$$

It follows from (6) and (1) that I is minimized when the following condition is satisfied

$$\mathbb{I}_n^{(i)} \subseteq \mathbb{I}_{n'}^{(i)} \quad \forall n \in \mathcal{N}_m, \quad (2)$$

for $m = 1, \dots, M$ and $i \in \{1, 2\}$. Equation (2) implies that $\mathbb{I}_{n'}^{(i)} = \bigcup_{n \in \mathcal{N}_m} \mathbb{I}_n^{(i)}$.

Assuming that the spectrum access strategy (2) is employed, we further show that

$$\mathbb{I}_n^{(i)} = \mathbb{I}_{n'}^{(i)} \quad \forall n \in \mathcal{N}_m, \quad (3)$$

and therefore $\theta_n^{(i)} = \hat{\theta}_m^{(i)} = \max\{\theta_n^{(i)}, n \in \mathcal{N}_m\} \quad \forall n \in \mathcal{N}_m$, for $m = 1, \dots, M$ and $i \in \{1, 2\}$. Suppose that (3) does not hold true, and there exists a sub-channel $k \in \mathcal{N}_m$ satisfying $\theta_k^{(i)} < \hat{\theta}_m^{(i)}$. Then, one can increase $\theta_k^{(i)}$ such that $\mathbb{I}_k^{(i)} = \mathbb{I}_{n'}^{(i)}$ ($\theta_k^{(i)} = \hat{\theta}_m^{(i)}$); this will increase R_{CRN} in (2) while not changing the values of I in (6) due to (2). This implies that one can further scale down $\theta_n^{(i)}$ for all $n \in \mathcal{N}_m$ to reduce I and R_{CRN} simultaneously, until $R_{CRN} = R_{\min}$. In summary, if (3) is not true, then one can always achieve a smaller objective value I for (P). Thus the optimal spectrum access strategy is given by (3).

Following the arguments in [19, Lemma 1], one can further show that if $x_m = 0$, then the optimal transmission times are given by $\mathbb{I}_n^{(1)} = [0, \hat{\theta}_m^{(1)} T_f]$ and $\mathbb{I}_n^{(2)} = [\alpha T_f, (\alpha + \hat{\theta}_m^{(2)}) T_f]$ for all $n \in \mathcal{N}_m$, and if $x_m = 1$, then the optimal transmission time intervals are given by $\mathbb{I}_n^{(1)} = [(\alpha - \hat{\theta}_m^{(1)}) T_f, \alpha T_f]$ and $\mathbb{I}_n^{(2)} = [(1 - \hat{\theta}_m^{(2)}) T_f, T_f]$ for all $n \in \mathcal{N}_m$. Lemma 1 is thus proved. ■

REFERENCES

- [1] Q. Zhao and B. M. Sadler, "A survey of dynamic spectrum access: Signal processing, networking, and regulatory policy," *IEEE Signal Process. Mag.*, vol. 24, no. 5, pp. 79–89, May 2007.
- [2] J. Peha, "Sharing spectrum through spectrum policy reform and cognitive radio," *Proc. IEEE*, vol. 97, no. 4, pp. 708–719, Apr. 2009.
- [3] V. Chandrasekhar, J. G. Andrews, and A. Gatherer, "Femtocell networks: A survey," *IEEE Commun. Mag.*, vol. 46, no. 9, pp. 59–67, Sep. 2008.
- [4] L. Law, K. Pelechrinis, S. Krishnamurthy, and M. Faloutsos, "Downlink capacity of hybrid cellular ad hoc networks," *IEEE/ACM Trans. Netw.*, vol. 18, no. 1, pp. 243–256, Feb. 2010.
- [5] D. Hu, S. Mao, Y. Hou, and J. Reed, "Scalable video multicast in cognitive radio networks," *IEEE J. Sel. Areas Commun.*, vol. 28, no. 3, pp. 334–344, Apr. 2010.
- [6] H. Kim and K. Shin, "Understanding Wi-Fi 2.0: From the economical perspective of wireless service providers," *IEEE Wirel. Commun. Mag.*, vol. 17, no. 4, pp. 41–46, Aug. 2010.
- [7] Q. Zhao, L. Tong, A. Swami, and Y. Chen, "Decentralized cognitive MAC for opportunistic spectrum access in ad hoc networks: A POMDP framework," *IEEE J. Sel. Areas Commun.*, vol. 25, no. 3, pp. 589–600, Apr. 2007.
- [8] H. Su and X. Zhang, "Cross-layer based opportunistic MAC protocols for QoS provisionings over cognitive radio wireless networks," *IEEE J. Sel. Areas Commun.*, vol. 26, no. 1, pp. 118–129, Jan. 2008.
- [9] S. Geirhofer, L. Tong, and B. M. Sadler, "Dynamic spectrum access in the time domain: Modeling and exploiting whitespace," *IEEE Commun. Mag.*, vol. 45, no. 5, pp. 66–72, May 2007.
- [10] —, "Cognitive medium access: Constraining interference based on experimental models," *IEEE J. Sel. Areas Commun.*, vol. 26, no. 1, pp. 95–105, Jan. 2008.
- [11] Q. Zhao, S. Geirhofer, L. Tong, and B. M. Sadler, "Opportunistic spectrum access via periodic channel sensing," *IEEE Trans. Signal Process.*, vol. 56, no. 2, pp. 785–796, Feb. 2008.
- [12] S. Geirhofer, J. Z. Sun, L. Tong, and B. M. Sadler, "Cognitive frequency hopping based on interference prediction: Theory and experimental results," *ACM SIGMOBILE Mob. Comput. and Commun. Rev.*, vol. 13, no. 2, pp. 49–61, Apr. 2009.
- [13] X. Li, Q. C. Zhao, X. Guan, and L. Tong, "Optimal cognitive access of Markovian channels under tight collision constraints," *IEEE J. Sel. Areas Commun.*, vol. 29, no. 4, pp. 746–756, Apr. 2011.
- [14] L. Lai, H. El Gamal, H. Jiang, and H. Poor, "Cognitive medium access: Exploration, exploitation, and competition," *IEEE Trans. Mob. Comput.*, vol. 10, no. 2, pp. 239–253, Feb. 2011.
- [15] P. Wang, M. Zhao, L. Xiao, S. Zhou, and J. Wang, "Power allocation in OFDM-based cognitive radio systems," in *Proceedings of Global Telecommunications Conference (IEEE GLOBECOM 2007)*, Nov. 2007, pp. 4061–4065.
- [16] R. Zhang and Y.-C. Liang, "Exploiting multi-antennas for opportunistic spectrum sharing in cognitive radio networks," *IEEE J. Sel. Topics Signal Process.*, vol. 2, no. 1, pp. 88–102, Feb. 2008.
- [17] A. Marques, X. Wang, and G. Giannakis, "Dynamic resource management for cognitive radios using limited-rate feedback," *IEEE Trans. Signal Process.*, vol. 57, no. 9, pp. 3651–3666, Sep. 2009.
- [18] R. Zhang, Y.-C. Liang, and S. Cui, "Dynamic resource allocation in cognitive radio networks," *IEEE Signal Process. Mag.*, vol. 27, no. 3, pp. 102–114, May 2010.
- [19] S. Geirhofer, L. Tong, and B. M. Sadler, "A sensing-based cognitive coexistence method for interfering infrastructure and ad-hoc systems," *Wirel. Commun. Mob. Comput.*, vol. 10, no. 1, pp. 16–30, Jan. 2010.

- [20] K. Huang, V. Lau, and Y. Chen, "Spectrum sharing between cellular and mobile ad hoc networks: Transmission-capacity trade-off," *IEEE J. Sel. Areas Commun.*, vol. 27, no. 7, pp. 1256–1267, Sep. 2009.
- [21] A. Høst-Madsen and J. Zhang, "Capacity bounds and power allocation for wireless relay channels," *IEEE Trans. Inf. Theory*, vol. 51, no. 6, pp. 2020–2040, Jun. 2005.
- [22] Y. Liang, V. V. Veeravalli, and H. V. Poor, "Resource allocation for wireless fading relay channel: Max-min solution," *IEEE Trans. Inf. Theory*, vol. 53, no. 10, pp. 3432–3453, Oct. 2007.
- [23] L. Vandendorpe, R. Duran, J. Louveaux, and A. Zaidi, "Power allocation for OFDM transmission with DF relaying," in *IEEE International Conference on Communications (ICC 2008)*, May 2008, pp. 3795–3800.
- [24] L. Vandendorpe, J. Louveaux, O. Oguz, and A. Zaidi, "Rate optimized power allocation for DF-relayed OFDM transmission under sum and individual power constraints," *Eurasip Journal on Wireless Communications and Networking*, Article ID 814278, doi:10.1155/2009/814278. pp. 1-9, Mar. 2009.
- [25] S. I. Resnick, *Adventures in Stochastic Processes*. Boston, MA: Birkhäuser, 1992.
- [26] B. H. Walke, S. Mangold, and L. Berlemann, *IEEE 802 Wireless Systems: Protocols, Multi-Hop Mesh/Relaying, Performance and Spectrum Coexistence*. Hoboken, NJ: John Wiley & Sons Inc., 2006.
- [27] F. H. P. Fitzek and M. Katz, "Cellular controlled peer to peer communications: Overview and potentials," in *Cognitive Wireless Networks*. Springer, Netherlands: Springer, 2007, pp. 31–59.
- [28] J. Mölsä, J. Karsikas, A. Kärkkäinen, R. Kettunen, and P. Huttunen, "Field test results and use scenarios for a WiMAX based Finnish broadband tactical backbone network," in *Proceedings of IEEE Military Communications Conference (IEEE MILCOM 2010)*, Oct. 31-Nov. 3, 2010, pp. 2357–2362.
- [29] A. E. Gamal and Y.-H. Kim, "Lecture notes on network information theory," 2010. [Online]. Available: <http://arxiv.org/abs/1001.3404>
- [30] S. Boyd and L. Vandenberghe, *Convex Optimization*. Cambridge, UK: Cambridge University Press, 2004.
- [31] S. A. Jafar and S. S. (Shitz), "Degrees of freedom region of the MIMO X channel," *IEEE Trans. Inf. Theory*, vol. 54, no. 1, pp. 151–170, Jan. 2008.
- [32] M. Chiang, S. Low, A. Calderbank, and J. Doyle, "Layering as optimization decomposition: A mathematical theory of network architectures," *Proc. IEEE*, vol. 95, no. 1, pp. 255–312, Jan. 2007.
- [33] D. P. Bertsekas, *Nonlinear Programming*, 2nd ed. Belmont, MA: Athena Scientific, 1999.
- [34] S. Boyd, L. Xiao, and A. Mutapic, "Lecture notes of ee392o: Subgradient methods," Stanford University, 2003. [Online]. Available: <http://www.stanford.edu/class/ee392o>
- [35] M. Bazaraa, H. Sherali, and C. Shetty, *Nonlinear Programming: Theory and Algorithms*, 3rd ed. Hoboken, New Jersey: Wiley-Interscience, 2006.
- [36] N. Z. Shor, *Minimization Methods for Non-Differentiable Functions*. New York, NY: Springer-Verlag New York, Inc., 1985.
- [37] J. Tang and X. Zhang, "Cross-layer resource allocation over wireless relay networks for quality of service provisioning," *IEEE J. Sel. Areas Commun.*, vol. 25, no. 5, pp. 645–656, May 2007.
- [38] Y. Zhang, S. Liu, Y. Rui, S. Zhou, and J. Wang, "Channel prediction assisted by radio propagation environments information," in *Proc. IEEE Int. Conf. Circuits Syst. Commun. (IEEE ICCSC)*, Shanghai, China, Feb. 2008, pp. 733–736.
- [39] S. Loyka and C. D. Charalambous, "On the compound capacity of a class of MIMO channels subject to normed uncertainty," *IEEE Trans. Inf. Theory*, accepted for publications, 2011.